PB83-168625

Electrostatic Augmentation of Fabric Filtration Pulse-Jet Pilot Unit Experience

Research Triangle Inst.
Research Triangle Park, NC

Prepared for

Industrial Environmental Research Lab.
Research Triangle Park, NC

Nov 82

U.S. Department of Commerce
National Technical Information Service
NTIS

PB83-168625

EPA-600/7-82-062
November 1982

ELECTROSTATIC AUGMENTATION OF FABRIC FILTRATION: PULSE-JET PILOT UNIT EXPERIENCE

by

D. W. VanOsdell and M. B. Ranade
Research Triangle Institute
P. O. Box 12194
Research Triangle Park, North Carolina 27709

G. P. Greiner and D. F. Furlong
ETS, Inc.
3140 Chaparral Drive, S. W.
Roanoke, Virginia 24018

EPA Contract No. 68-02-3186
RTI Project No. 47U-1915

Project Officer
L. S. Hovis
Industrial Environmental Research Laboratory
Office of Research and Development
U. S. Environmental Protection Agency
Research Triangle Park, North Carolina 27711

Prepared for

INDUSTRIAL ENVIRONMENTAL RESEARCH LABORATORY
OFFICE OF RESEARCH AND DEVELOPMENT
U. S. ENVIRONMENTAL PROTECTION AGENCY
RESEARCH TRIANGLE PARK, NORTH CAROLINA 27711

REPRODUCED BY
NATIONAL TECHNICAL
INFORMATION SERVICE
U.S. DEPARTMENT OF COMMERCE
SPRINGFIELD, VA. 22161

TECHNICAL REPORT DATA
(Please read Instructions on the reverse before completing)

1. REPORT NO. EPA-600/7-82-062	2.
3. RECIPIENT'S ACCESSION NO. PB83 168625	
4. TITLE AND SUBTITLE Electrostatic Augmentation of Fabric Filtration: Pulse-jet Pilot Unit Experience	5. REPORT DATE November 1982
	6. PERFORMING ORGANIZATION CODE
7. AUTHOR(S) D. W. Van Osdell, M. B. Ranade, G. P. Greiner*, and D. F. Furlong* (* = ETS, Inc.)	8. PERFORMING ORGANIZATION REPORT NO. 47U-1915
9. PERFORMING ORGANIZATION NAME AND ADDRESS Research Triangle Institute P.O. Box 12194 Research Triangle Park, North Carolina 27709	10. PROGRAM ELEMENT NO.
	11. CONTRACT/GRANT NO. 68-02-3186
12. SPONSORING AGENCY NAME AND ADDRESS EPA, Office of Research and Development Industrial Environmental Research Laboratory Research Triangle Park, NC 27711	13. TYPE OF REPORT AND PERIOD COVERED Final; 10/79-2/81
	14. SPONSORING AGENCY CODE EPA/600/13

15. SUPPLEMENTARY NOTES IERL-RTP project officer is Louis S. Hovis, Mail Drop 61, 919/541-2925.

16. ABSTRACT The report describes the development of the parallel-field electrostatically augmented fabric filter (ESFF) on a pilot-scale pulse-cleaned baghouse. The pilot unit consisted of parallel conventional and ESFF baghouses installed on a slipstream from a pulverized-coal boiler. Teflon and fiberglass fabrics were investigated under a wide variety of operating conditions. Major parameters studied were particulate collection (total mass and size dependent), baghouse pressure drop, and electrical characteristics. Research results show that the ESFF baghouse has significant advantages over conventional ones. The flow resistance of the collected dust is substantially reduced. Under the same operating conditions, an ESFF baghouse has about half the pressure drop of a conventional one. Alternatively, the flow through a given area of fabric (face velocity) can be increased at constant pressure drop in the ESFF baghouse. Experience at the ESFF pilot unit suggests that face velocity can be doubled. An economic projection based on these results indicates that the ESFF would reduce the annualized cost of the filter by 30 percent. Particulate control capabilities of the ESFF baghouse were about the same as for the conventional one, with outlet loadings averaging less than 0.017 g/std cu m.

17. KEY WORDS AND DOCUMENT ANALYSIS

a. DESCRIPTORS	b. IDENTIFIERS/OPEN ENDED TERMS	c. COSATI Field/Group
Pollution Filtration Fabrics Electrostatics Tetrafluoroethylene Resins Glass Fibers Dust Aerosols	Pollution Control Stationary Sources Fabric Filters Baghouses Particulate	13B 11G 07D 11E 20C 11I

18. DISTRIBUTION STATEMENT Release to Public	19. SECURITY CLASS (This Report) Unclassified	21. NO. OF PAGES 99
	20. SECURITY CLASS (This page) Unclassified	22. PRICE

EPA Form 2220-1 (9-73)

NOTICE

This document has been reviewed in accordance with U.S. Environmental Protection Agency policy and approved for publication. Mention of trade names or commercial products does not constitute endorsement or recommendation for use.

ABSTRACT

This report describes the development of the parallel field electrostatically augmented fabric filter (ESFF) on a pilot-scale pulse-cleaned baghouse. The pilot unit consisted of parallel conventional and ESFF baghouses installed on a slipstream from a pulverized coal boiler. Both Teflon® and fiberglass fabrics were investigated under a wide variety of operating conditions. The major parameters studied were particulate collection (total mass and size dependent), baghouse pressure drop, and electrical characteristics.

The results of this research show that the ESFF baghouse has significant advantages over conventional technology. The flow resistance of the collected dust is substantially reduced. Under the same operating conditions, an ESFF baghouse has about half the pressure drop of a conventional baghouse. Alternatively, the flow through a given area of fabric (face velocity) can be increased at constant pressure drop in the ESFF baghouse. Experience at the ESFF pilot unit suggests that a doubling of face velocity is possible. An economic projection based on these results indicates that with the ESFF 30 percent reduction in the annualized cost of the filter would be achieved. Particulate control capabilities of the ESFF baghouse were about the same as for the conventional baghouse, with the outlet loadings averaging less than 0.017 g/sm^3.

EXECUTIVE SUMMARY

INTRODUCTION

The deliberate use of electrostatic forces to enhance the operation of a fabric filter has been the subject of research for some time. Several concepts have been proposed and tested to some degree. Work partially supported by the U. S. Environmental Protection Agency led to the development of an electrostatic augmentation concept which utilized an electric field parallel to the fabric surface, did not utilize particle charging, and was physically similar to conventional pulse-jet fabric filters. The enhancement obtained over conventional fabric filtration was manifested most clearly as a reduction in the flow resistance of a given mass of collected dust. An improvement in dust collection efficiency was also noted in the laboratory.

The primary objective of this research program was to evaluate this concept of electrostatic augmentation of fabric filtration (ESFF) at pilot-scale on a slipstream from a coal-fired boiler. This required that a pilot plant be designed, constructed, and operated. Secondary objectives of the work were to evaluate performance with respect to particle size, estimate the effects of different coal types, and evaluate the economics of the ESFF system.

SCOPE

A pilot baghouse facility, consisting of parallel conventional (control) and ESFF baghouses, a control house, and required gas-handling equipment, was constructed. The parallel test and control baghouses were very important to the test program, allowing conclusions to be drawn rapidly without fear of underlying "history" effects. The baghouses were checked to ensure identical inlets. Each baghouse was about the size of the smallest commercial pulse-jet baghouses, roughly 1 m square by 5 m high. Cleaning was by a conventional pulse-jet system operating at typical energy levels [50-ms pulse of 650 to 790 kPa (80 to 100 psia) air]. The baghouses were designed for volumetric

flow rates of 8.5 to 14.2 m^3/min (300 to 500 cfm). The bags utilized were 11.4 cm (4.5 in.) in diameter by 244 cm (8 ft) long. Face velocity in the baghouses was varied from 1 to 5 cm/s (2 to 10 ft/min) through flow control and blanking off bags as necessary. Up to five bags were used in each baghouse. Normal operation was continuous, 24 hours each day, during a test program.

The flue gas slipstream controlled by the pilot plant was from an industrial pulverized coal boiler. The average inlet mass loading was 0.7 g/m^3 (0.3 gr/scf). Inlet temperatures at the pilot baghouse were about 150° C. The coals burned in the boilers were highly variable. Sulfur content ranged from 0.6 to 1.9 percent (average about 1.3 percent) and ash content from 6 to 27 percent (average of about 13 percent).

The electrical hardware consisted of high voltage DC power supplies, current and voltage instrumentation, and the ESFF electrodes. The electrodes initially used consisted of an array of thin wire electrodes, oriented vertically on the outside (dirty-gas-side) of the bag and tied to the outside of the bag. The wires were alternately charged to a relative potential difference of between 0 and up to about 10 kV. Spacing between electrodes varied from about 1.5 to 2 cm. A cage/electrode assembly was developed and proved to overcome the difficulties inherent in the wire harness. The cage electrode replaced the usual pulse-jet bag cage on the inside (clean-gas-side) of the bag.

The fabrics used during most of this test program were three types of felted Teflon®, including the commercial 23-oz felt. A woven glass fabric (texturized in the fill yarn) was also tested for a short time. The surface quality of the fabric (smooth or fuzzy) was an important parameter during the laboratory work. Less dense surfaces resulted in greater enhancement.

RESULTS AND DISCUSSION

The most important results obtained at the ESFF pilot unit were associated with a reduction in the pressure drop required to operate a fabric filter. Three aspects of this improvement over conventional technology were noted: (1) a reduction in the flow resistance of the collected dust, (2) a reduction in the residual pressure drop of the filter (the pressure drop of a

"just-cleaned" filter), and (3) a capability to operate at higher face velocities without blinding (uncontrollable increase in average pressure drop).

The reduction in the resistance of the dust cake to flow was the primary effect noted in the laboratory, and the pilot unit confirmed this effect. The ratio of the pressure drop increase of the ESFF baghouse to that of the conventional baghouse over one cleaning cycle was used as a measure of this effect. As the two baghouses were exposed to the same mass flow rate of dust for the same length of time, the difference in pressure drop increase must be due to a reduction in the flow resistance of the dust cake in the ESFF baghouse. At a field strength of 1 kV/cm, the pressure drop ratio (PDR) was about 0.56, at 3 kV/cm the PDR was 0.37, and at 5 kV/cm it was about 0.26. These results are in the same range as the laboratory results.

In addition, the residual pressure drop (ΔP_r) of the ESFF baghouse was found to be less than that of the conventional baghouse. For one consistent set of tests, the ESFF baghouse ΔP_r was about 60 percent of that for the control baghouse. There was considerable scatter in the data, and it was not possible to correlate the ΔP_r reduction with operating parameters.

It was possible to operate the ESFF baghouse at steady-state at higher face velocities than was possible in the control baghouse. Pulse-jet baghouses on boilers typically can operate at a face velocity of around 2 cm/s (4 ft/min). Operation at much above 2 cm/s (4 ft/min) leads to an uncontrollable increase in pressure drop (blinding). The pilot conventional baghouse operated in this way. Stable operation was possible up to 10 cm/s (5 ft/min), but blinding occurred at higher face velocities. The ESFF baghouse, on the other hand, operated for extended periods at 6 and 8 ft/min and for a short run at 10 ft/min, without blinding.

The increase in baghouse capacity possible at increased face velocities gives the ESFF baghouse an economic advantage over conventional technology. The added costs due to the ESFF hardware and operating expenses are relatively minor. An ESFF baghouse operated at 3 cm/s (6 ft/min) was estimated to have a total annual cost about 30 percent below that of a conventional baghouse operated at the more common 2 cm/s (4 ft/min). Sill higher face

velocities lead to even greater savings. The figures above are based on pulse-jet baghouse control of a 27,200 Kg steam/hr (60,000 lb/hr) pulverized coal industrial boiler.

During this work, the particulate control capabilities of the ESFF baghouse were about the same as for the conventional baghouse.

The Research Triangle Institute (RTI) as the prime contractor provided overall project management and electrostatic hardware design and construction. ETS, Inc., as the principal subcontractor, designed, constructed, and operated the pilot unit. The Textile Research Institute (TRI) acted as a design consultant and provided fabric evaluation on their bench-scale equipment.

This report was submitted in fulfillment of Contract No. 68-02-3186 by the Research Triangle Institute under the sponsorship of the U. S. Environmental Protection Agency. This report covers the period from October 1979 to February 1981. Work under this contract is continuing with the evaluation of a reverse-air-cleaned baghouse augmented with ESFF.

TABLE OF CONTENTS

	Page
Abstract	ii
Executive Summary	iii
List of Figures	ix
List of Tables	x
Acknowledgments	xi
1. Introduction	1
2. Conclusions	3
3. Recommendations	4
4. Background	5
Introduction	5
Electrostatic Forces	5
Coulombic Force	6
Image Charge Force	6
Dielectrophoresis	8
Electrostatic Enhancement: Concepts and Methods	11
TRI Concept of Electrostatic Enhancement	15
5. Pulse-Jet Pilot Unit	19
Introduction	19
Dust Source	19
Pilot Baghouses and Test Trailer	21
Electrical Hardware	25
6. Operation	30
Introduction	30
Break-In Period--Modifications	30
Initial Test Series: Mid-June Through Mid-July 1980	34
Second Test Series	35
Third Test Series	35
Fourth Test Series	38
Experience with Electrical Hardware	38
7. Results	41
Introduction	41
Dust Cake	41
Dust Cake Flow Resistance	44
Reduced Residual Pressure Drop	49
Operation at Increased Face Velocity	49

Preceding page blank

TABLE OF CONTENTS (continued)

	Page
Particulate Removal Efficiency	53
Fabric Effects	59
Electrical Requirements	62
8. Economics	63
Introduction	63
Analytical Methods	63
Results	68
References	75
Appendices	
A. Impactor Test Procedures	77
B. Charge-To-Mass Measurement Operating Procedure	83

LIST OF FIGURES

		Page
Figure 1.	Schematic diagram of the image charge effect.	7
Figure 2.	Dielectrophoresis	9
Figure 3.	APITRON design and operation.	13
Figure 4.	Laboratory apparatus for fabric filtration in an electric field oriented perpendicularly to the fabric	14
Figure 5.	Harness for applying electric field parallel to the surface of a fabric filter bag.	14
Figure 6.	Modification of electric field by fibers or particles	16
Figure 7a.	Average PDR results from TRI bench-scale work	18
Figure 7b.	Average penetration results from TRI bench-scale work	18
Figure 8.	Schematic diagram of ESFF pulse-jet pilot unit.	22
Figure 9.	Isometric drawing of pilot unit baghouses	23
Figure 10.	High voltage ESFF electrical circuit.	26
Figure 11.	Inside electrodes utilizing insulating ring spacers	28
Figure 12.	Inside electrodes utilizing insulating tubing on cage rings	29
Figure 13.	Waynesboro fly ash resistivity.	45
Figure 14.	Pressure drop plot for pilot baghouse	47
Figure 15.	PDR-field strength relationship for Teflon® and glass fabrics	48
Figure 16.	Pressure drop ratio as a function of field strength and face velocity.	50
Figure 17.	Residual pressure drop for ESFF and control baghouse.	51
Figure 18.	Residual pressure drop at two face velocities	52
Figure 19a.	Residual pressure drop for January 12-18, 1981.	54
Figure 19b.	Residual pressure drop for January 19-25, 1981.	55
Figure 19c.	Residual pressure drop for January 26-28, 1981.	56
Figure 20.	Inlet mass concentration comparison for ESFF and control baghouses	58
Figure 21.	Inlet and outlet cumulative size distributions.	60

LIST OF FIGURES (continued)

		Page
Figure 22.	Average size-dependent particle penetration	61
Figure 23.	Pulse-jet baghouse cost: pulverized coal industrial boiler	72
Figure 24.	Reverse-air baghouse cost: power plant	74

LIST OF TABLES

		Page
Table 1.	Electrical Forces Between a Spherical Particle and a Cylindrical Fiber	11
Table 2.	Waynesboro, Virginia, Boiler House	20
Table 3.	Pilot Unit Features	24
Table 4.	Summary of ESFF Pulse-Jet Pilot Unit Test Program	31
Table 5.	Third Test Series Operating Conditions	37
Table 6.	History of Fourth Test Series	39
Table 7.	Bulk Density of Collected Fly Ash	43
Table 8.	Particulate Charge-To-Mass Ratio	46
Table 9.	Method 5 Test Results	57
Table 10.	Installed Cost Factors as a Function of Equipment Cost Q	65
Table 11.	Cost Estimate for a Pulse-Cleaned Baghouse Having 225 15.24-cm (6-in.) Diameter by 4.3-m (14-ft) Bags (460 m^2 of cloth)	66
Table 12.	Conventional Pulse-Jet Baghouse--Equipment Cost \$161.50/m^2	69
Table 13.	ESFF Pulse-Jet Baghouse--Equipment Cost \$183/m^2	70
Table 14.	Reverse-Air Baghouse--Total Annual Cost, \$/(m^3/min)-yr	71

ACKNOWLEDGMENTS

The assistance provided by E. I. du Pont de Nemours and Company, Inc., is gratefully acknowledged. The pilot unit was located at Du Pont's Waynesboro, Virginia, plant, and the power plant personnel under the direction of Mr. Otis Bilkins have been very helpful. In addition, Teflon® fabric was provided to the program by Du Pont through Mr. Jack Shah.

Mr. Jim Abbott, former Head of the Particulate Technology Branch, and Dr. Louis Hovis, Project Officer, were closely involved in the project and provided guidance and assistance.

SECTION 1

INTRODUCTION

The use of fabric filters to remove particles from gas streams is well established in industrial practice and of growing importance for electrical utility boilers. For utility boilers, the fabric filter has an advantage over other particulate control equipment with respect to removal efficiency. It is roughly competitive in price. However, fabric filtration operating experience on utility boilers is limited, and enough questions have been raised by unexpectedly high baghouse pressure drops to cause caution in the industry.

A concept of electrostatically augmented fabric filtration (ESFF) was developed by the Textile Research Institute (TRI) through laboratory work partially supported by EPA. This concept has potential for significant improvements in fabric filter performance. Laboratory work at TRI and reports in the literature indicate that an electric field will modify the dust deposit. While visually the dust deposit appears unchanged, a given areal density of dust on the bag exhibits reduced pressure drop at a given flow rate. This change in the specific dust cake flow resistance (reduced drag per unit areal density) has been demonstrated consistently. In addition, the laboratory work indicates that the pressure drop of the cleaned fabric (residual pressure drop) might be reduced.

This project required that the laboratory and bench-scale work discussed above be transferred to pilot-scale hardware and operated in a field environment. The economics of the process were then to be evaluated. The successful results of this effort are reported in the following sections. Section 4 discusses the background literature pertinent to ESFF, including a brief presentation of the forces involved, selected portions of the literature, and the developmental work done at TRI. Section 5 is a description of the pilot unit and associated equipment, and Section 6 is a summary of operating experience

and test procedures at the pilot unit. Section 7 is a presentation of the results of the pilot unit investigation. The economic evaluation of the process is given in Section 8.

The work reported here is all from pulse-cleaned baghouse operation. Electrostatic augmentation of reverse-air-cleaned baghouses will be studied in the second phase of this program.

SECTION 2

CONCLUSIONS

Electrostatic augmentation of fabric filtration (ESFF) utilizing an electric field parallel to the fabric surface (with no particle charging) has been successfully applied at pilot scale on a pulse-jet baghouse.

The electrode configuration developed in the course of this study consists of a combination cage/electrode assembly, modified from a conventional pulse-jet cage, and appears to be a design with potential for commercial use.

At any given face velocity, the pilot ESFF baghouse had a reduced residual pressure drop and a reduced rate of pressure drop increase when compared to the pilot conventional baghouse.

The pilot ESFF baghouse could be operated in a stable fashion at face velocities up to about twice the stable operating conditions possible for the pilot conventional baghouse.

A reduction in total annualized cost of 30 percent or more was estimated for a typical industrial boiler installation which was controlled by an ESFF pulse-jet baghouse at 3 cm/s rather than a conventional pulse-jet baghouse at 2 cm/s. For a 27,200-kg-steam/hr (60,000 lb/hr) boiler using electricity at $0.05/kWh, the estimated annualized cost of the ESFF baghouse was about $107,000 at 3 cm/s, while the cost of a conventional baghouse at 2 cm/s was estimated to be $146,000/yr.

Particulate mass emissions from the two pilot baghouses were not significantly different. The average efficiency for the pilot ESFF baghouse was 98 percent, with an average outlet loading of 0.17 g/sm^3. The average efficiency of the pilot conventional baghouse was 98.9 percent, with an average outlet loading of 0.016 g/sm^3.

SECTION 3

RECOMMENDATIONS

A program to install pulse-jet ESFF at essentially full commercial scale should be undertaken. The retrofit of a single compartment of an existing pulse-jet baghouse with ESFF or the modification of a new design would be sufficient. This program should be directed toward investigating system scale-up parameters and an extended (months-long) period of routine testing.

The use of ESFF with fabrics other than the felted Teflon® and woven fiberglass tested in this program should be investigated. Laboratory work indicates that other fabrics can be used as ESFF fabrics, and in some applications these might be desirable.

An investigation of the use of ESFF on dust sources other than pulverized coal-fired boilers is recommended. The advantages of ESFF should be applicable to other sources, but little data is available.

The importance of fabric-dust interactions and properties should be investigated. This would include the electrical properties of both the fabric and the dust, particle size, natural charge of the dust, gas conditions, and similar parameters.

SECTION 4

BACKGROUND

INTRODUCTION

The use of electrostatic phenomena to improve the performance of conventional fabric filters has only recently been attempted for commercial application. Conventional design practice does not consider the electrical properties of the dust or the fabric. Research has shown, however, that the electrostatic forces on particles in a fabric filter can be important, and their importance can be increased by introducing charge on the particles or by applying an external electric field. The work discussed in this report is the application of a particular electrostatic enhancement concept to fabric filtration of coal-fired boiler flue gas. The sections below outline: (1) the forces which are thought to be important, (2) some concepts which make use of these forces to improve filter performance, and (3) the particular concept on which this work was based.

ELECTROSTATIC FORCES

Electrical charges existing anywhere in a fabric filter have electrical fields associated with them that influence the entire system. Externally applied electric fields over and above those created by the discrete charges of the system also contribute to the total electric field. In principle, the electrostatics problem can be solved for any collection of charges and fields by rigorous use of Maxwell's equations; in practice, the complexity of the problem and lack of sufficient data concerning charge magnitude, location, and system properties make rigorous solution unlikely.

Analogy with some simple, solvable, special cases, however, can provide insight as to what kinds of interactions are occurring and can permit qualitative predictions of electrical effects in real systems. The discussion below is based on a single-fiber/single-particle system. Three interactions are significant:

1. The Coulombic force,

2. The image charge force, and

3. Dielectrophoresis.

Coulombic Force

Coulomb's Law gives the force between two point charges. Alternatively, it can be written as the influence of the electric field of one point charge upon the other. By superposition of all point charge interactions, the net force field of a system of charges can be obtained. By extension of these concepts to charged particles and charged fibers, the Coulombic force describes the electrical force between two charged components of the system. Consider, for example, the Coulombic force between a spherical particle of charge, q_p, and a cylindrical fiber of Q charges/unit length. In air (dielectric constant = 1) the Coulombic force, F_c, is:

$$F_c = \frac{2Qq_p}{r} \qquad (1)$$

where r = the distance between the surface of the cylindrical fiber and the center of the particle.

The Coulombic force can be either attractive or repulsive, depending on the signs of Q and q_p. Coulombic forces generally dominate those systems in which they exist; they constitute the basis on which electrostatic precipitators operate. Repulsive Coulombic forces between charged particles of like sign produce a space charge force in unipolar dust flows.

Image Charge Force

Electrically neutral bodies placed in an electric field undergo internal charge displacements because of the electric field. In particular, the electrical charge on the spherical particle considered above creates an electric field which induces a charge redistribution in the adjacent cylindrical fiber (Figure 1). When applied to a spherical particle and cylindrical fiber, the image force becomes:

$$F_{i_c} = \frac{q_p^2}{4r^2} \qquad (2)$$

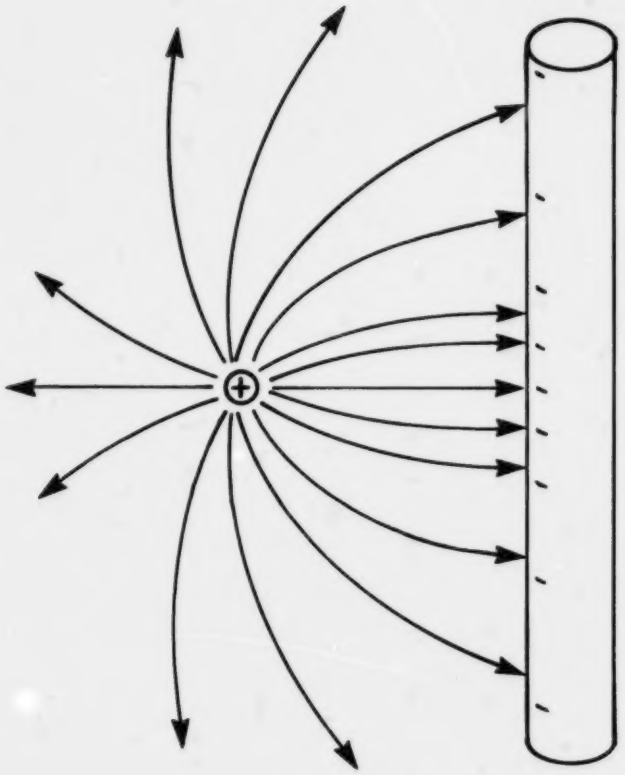

Figure 1. Schematic diagram of the image charge effect.

or, for a nonconductive fiber:

$$F_{i_{non}} = -\left(\frac{K_1 - 1}{K_1 + 1}\right) \frac{q_p^2}{4r^2}$$

where K_1 = the dielectric constant of the nonconducting fiber.

The negative sign of this force implies that the force is attractive. This conclusion holds regardless of the sign of the particle charge. The image force is an additional collecting force on a particle attributable to its electrical charge alone. Simply adding electrical charge to a dust creates an additional capture force for that particle in a dust collection device whether or not other charges exist in the system; the forces in Equations 2 and 3 depend only on q_p.

Dielectrophoresis

The reciprocal relationship to that just described is the influence of the electric field created by fiber charge on the charge distribution of a neutral particle. When the electric field causing the charge separation in the particle is not homogeneous, a net attractive force in the direction of increasing field strength is experienced by the electrically neutral particle. This effect, called dielectrophoresis, is illustrated in Figure 2. Since the negative charges on the particle in this illustration are displaced toward the region of higher field strength, they experience a greater Coulombic force than do the equal number of positive charges located in regions of lower electric field strength. A fiber in a fabric filter can become charged by the accumulation of charged dust or can appear charged due to charge displacement caused by an external electric field. In either case, the field will be complicated with multiple interactions from other fibers and baghouse hardware. As the particle nears a fiber, however, the situation begins to approach that shown in Figure 2. The result of dielectrophoresis is always a net force on the neutral particle toward the region of higher field strength regardless of field direction.

For a neutral spherical particle (in air) adjacent to a charged cylindrical fiber, the net attractive force is:

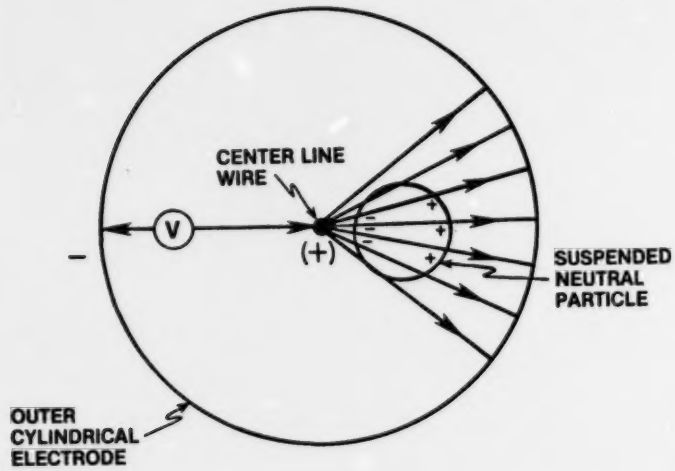

Figure 2. Dielectrophoresis.

$$F_d = -\left(\frac{K_2 - 1}{K_2 + 1}\right) \frac{D_p^3 Q^2}{2r^3} \qquad (4)$$

where K_2 = the dielectric constant of the particle, and

D_p = the particle diameter.

These three forces cover the three charged-particle charged-fiber combinations as summarized in Table 1.

TABLE 1. ELECTRICAL FORCES BETWEEN A SPHERICAL PARTICLE AND A CYLINDRICAL FIBER

Particle charge	Fiber charge/ unit length	Force
q_p	Q	$\frac{2Qq_p}{r}$ (Coulomb)
q_p	Q	$-\left(\frac{K_1 - 1}{K_1 + 1}\right) \frac{q_p^2}{4r^2}$ (Image)
0	Q	$-\left(\frac{K_2 - 1}{K_2 + 2}\right) \frac{D_p^3 Q^2}{2r^3}$ (Dielectrophoretic)

r = Distance between the surface of the cylindrical fiber and the center of the spherical particle.

D_p = Particle diameter.

K_1 = Dielectric constant of fiber.

K_2 = Dielectric constant of particle.

For this particular geometry, each of these forces depends on distance differently, the Coulombic force decreasing least rapidly with increasing

separation. Note, however, that there are regions and conditions under which any of the forces can dominate. These conditions can be determined by comparing the force expressions. For example, dielectrophoretic forces are predicted to exceed Coulomb forces when:

$$\left| \frac{K_2 - 1}{K_2 + 2} \frac{D_p^3}{r^2} \right| > \left| \frac{4q_p}{Q} \right| . \qquad (5)$$

For fixed particle properties and constant system charges, this condition is most likely to be fulfilled in the region adjacent to the fiber. Indeed, with appropriate values, the attractive dielectrophoretic force of a negatively charged fiber on a negatively charged particle can exceed the repulsive Coulombic force so that the net motion of the particle is still toward the fiber even though the like signs of the electrical charges on each particle intuitively suggest a repulsion.

With parameters typical of conventional fabric filtration, Coulombic forces dominate; dielectrophoretic forces are next in importance; and image forces are the least and are generally negligible.[1]

Problems more complex than the single spherical particle adjacent to a single cylindrical fiber have been modeled, such as the deposition of many particles on a single fiber.[2,3,4] These cases include particle charge and/or externally applied electric fields as variables. The modeling complexity falls short of adequately realistic simulation of dust cake growth even in the electrically neutral case. What is important to recognize is that a conceptual basis exists for expecting enhanced particle collection because of electrical forces so that empirical data can be interpreted and assessed in view of these expectations.

ELECTROSTATIC ENHANCEMENT: CONCEPTS AND METHODS

The equations presented above show that for a given dust and fiber, the electrostatic forces can be influenced by fiber charge per unit length, Q, and particle charge, q_p. Particles in a waste stream normally have some charge, although the sign and quantity of charge is not predictable. In like manner, fabric which is filtering a dirty gas stream acquires charge[5] and this charge influences particle collection.

Artificial control of particle charging is an obvious next step, a principle which has been used by researchers. A corona charger has been used to increase particle charge, and filter performance has been monitored. The APITRON is a commercial embodiment of this technique (Figure 3). Particles are charged in the entry thimble and collected on the bag. Ariman and Helfritch[7] have reported significant performance improvements using this equipment on various dusts and with various fabrics. Other recent research using a patch type of apparatus has been reported by Iinoya and Mori[8] and Chudleigh and Bainbridge.[9]

In the charged dust technique described above, the electric field in the vicinity of the fabric is thought to depend, initially, only on the space charge created by the incoming charged dust. As this charged dust is collected and a dust cake is built up on the fabric surface, the electrical properties of the fabric and the dust itself play a role in determining the local electric field at the fabric surface.

In contrast, it is possible to apply an external field near the fabric, increasing fiber charge and hence improving collection. This requires a specially designed electrode system positioned so as to create the desired electric field at the fabric surface.

One obvious method of applying an electric field across a fabric or fiber filter is to sandwich the fibers between two metallic screens which then serve as the electrodes for the external field. This technique is especially appropriate for fiber filters which often require mechanical support anyway.[10,11] Considerable analysis and experimentation has been carried out with fiber filters of various densities in electric fields of various orientations.[10,12,13]

Penney[14,15] used a short section of a bag fabric filter mounted on an inside support cage, which was electrically grounded (Figure 4). The entire assembly was then inserted inside a conductive cylinder which was electrically isolated from ground so that it could serve as the high voltage electrode as well as part of the filter housing.

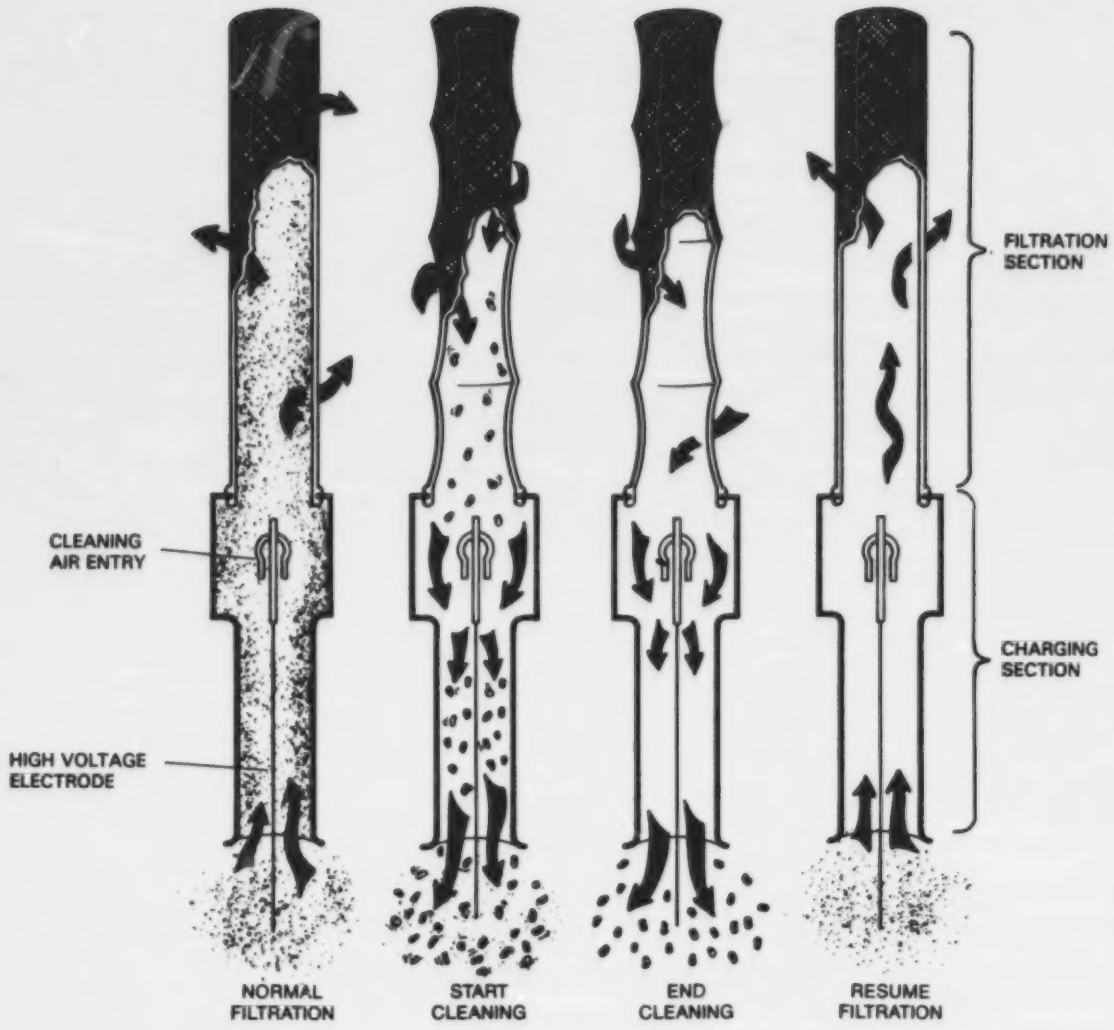

Figure 3. APITRON design and operation (Helfritch, 1979).

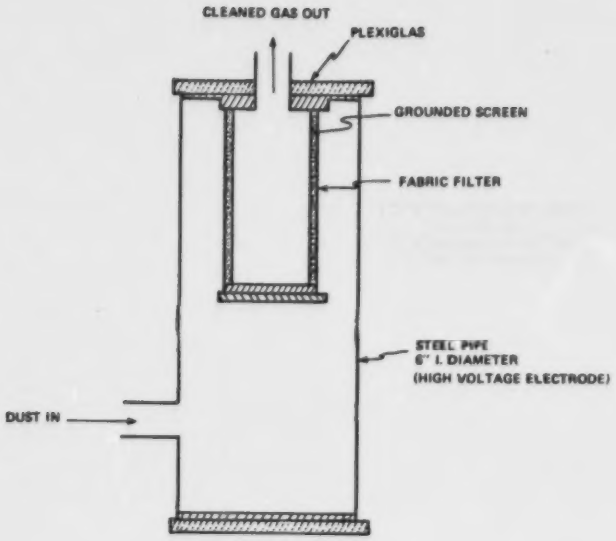

Figure 4. Laboratory apparatus for fabric filtration in an electric field oriented perpendicularly to the fabric.

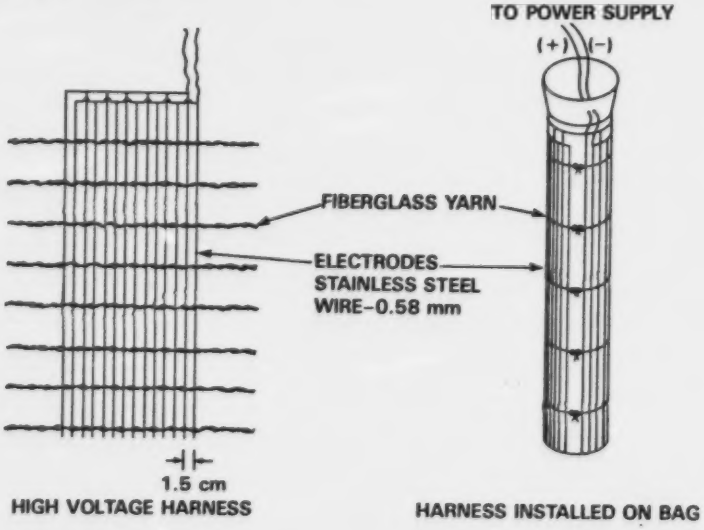

Figure 5. Harness for applying electric field parallel to the surface of a fabric filter bag.

In both the screen sandwich structure and the Penney configuration, the electric field is perpendicular to the fabric surface and along the direction of gas flow.

An alternative orientation was chosen by Lamb and Costanza [16,17,18] of Textile Research Institute (TRI) in their development of ESFF. Their configuration orients the electric field in the plane of the fabric surface, perpendicular to the direction of gas flow. A recent version of their laboratory hardware is illustrated in Figure 5.

Both these orientations (electric field perpendicular or parallel to flow) create converging electric fields in the vicinity of the fabric fibers or the dust particles already captured by the fibers, which in turn favors additional electrostatic capture at these same sites because of the electric field convergence. The field-fiber (or particle) interaction is sketched schematically in Figure 6 following Rivers'[13] analysis. The deposition sites favored by electrostatics are along the axis of the electric field whether the flow is parallel or perpendicular to the electric field. From the frame of reference of a fiber, these favored sites will be either the front and back of the fiber or the sides, depending on whether the flow is parallel or perpendicular to the electric field. This means the aerodynamic interaction in the two cases could be expected to be different. Theoretical calculations made by TRI led those workers to select the orientation with the field perpendicular to the gas flow as most advantageous.[17]

TRI CONCEPT OF ELECTROSTATIC ENHANCEMENT

The use of electric fields perpendicular to the gas flow (parallel to the fabric) was pursued by TRI both on a 10-cm-diameter flat filter apparatus and on a small ambient-temperature bench-scale baghouse. The field was applied using a harness similar to that presented in Figure 5. The work at TRI led to the following general guidelines for ESFF system design.

1. The electric field should be parallel to the fabric surface. The field could be effectively produced by an array of relatively fine wires on the dirty-gas side of the fabric. The wires should be in contact with but not incorporated into the fabric.

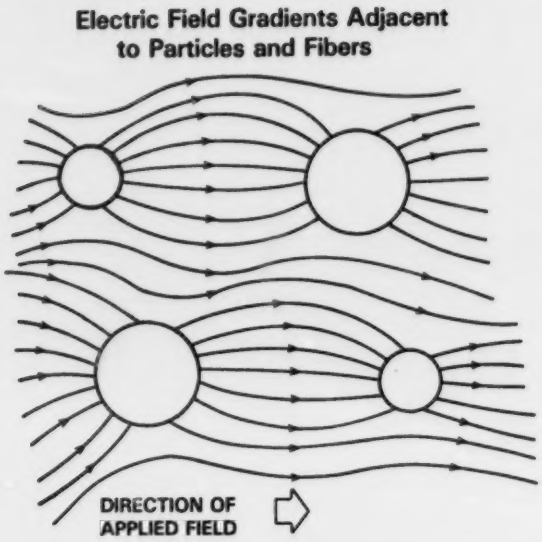

Figure 6. Modification of electric field by fibers or particles.

2. The degree of electrostatic enhancement obtained is strongly influenced by the surface characteristics of the fabric. A low density surface gives the best results.

3. The effect of the electrostatic augmentation is most obvious in reduced dust cake flow resistance and in reduced particle penetration.

In order to quantify the change in dust cake flow resistance, the pressure drop ratio (PDR) was defined as:

$$PDR = \frac{(\Delta P_f - \Delta P_r)_{ESFF}}{(\Delta P_f - \Delta P_r)_{control}} \qquad (6)$$

where ΔP = the pressure drop across the bags,

f = the final state (just prior to cleaning),

r = the residual state (just after cleaning), and

control = a baghouse without electrical enhancement.

For an idealized filter cycle in which the bag pressure drop increases linearly with time at constant dust loading from ΔP_r to ΔP_f, it can be shown that:

$$PDR = \frac{(K_2)_{ESFF}}{(K_2)_{control}} \qquad (7)$$

where K_2 = the specific cake resistance (drag per unit areal density).

PDR, then, is the ratio of the flow resistance of a dust cake collected by an ESFF system to that of a conventional fabric filter.

Results obtained by TRI using felted Teflon® fabric are presented in Figures 7a and 7b. These curves were obtained by averaging bench-scale unit data which were taken at four values of average electric field strength. Pilot unit results differed in several respects; the results are given in Section 7.

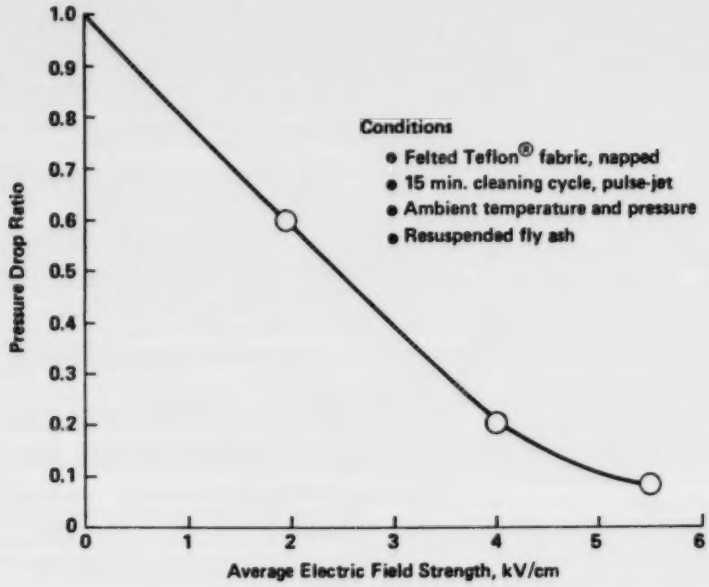

Figure 7a. Average PDR results from TRI bench-scale work (after Lamb and Costanza[17]).

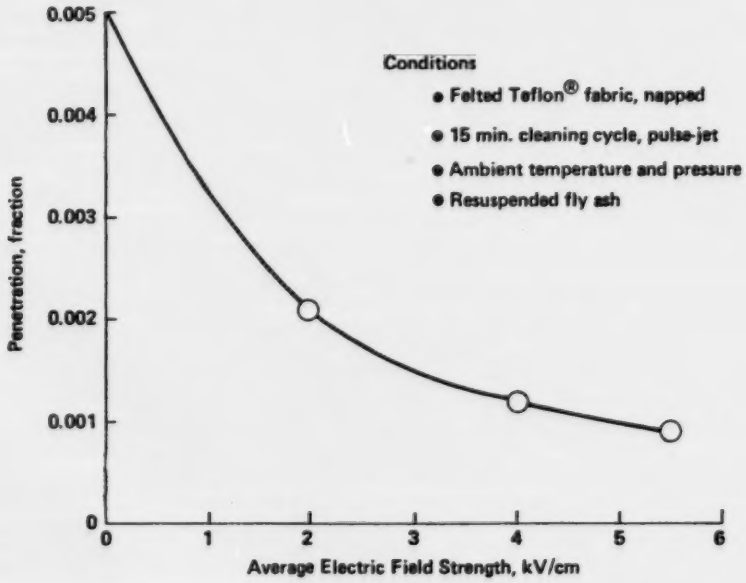

Figure 7b. Average penetration results from TRI bench-scale work (after Lamb and Costanza[17]).

SECTION 5

PULSE-JET PILOT UNIT

INTRODUCTION

The basis of the ESFF pilot unit test program was parallel operation of a conventional baghouse and an electrostatically augmented baghouse. Boiler and coal variations in an operating boiler were expected to be too large for successful testing to be done serially in time in a single baghouse. Operation of the pilot unit has borne out and even further emphasized the desirability of this approach. The following sections provide a description of the dust source, the pilot unit as constructed, and the electrical hardware installed.

DUST SOURCE

The pilot unit was operated on a slipstream from the boiler house of the Waynesboro, Virginia, Du Pont plant. Table 2 is a summary of the boiler house characteristics. The Waynesboro boiler house baghouse has been described by Marcotte.[19] The pilot unit slipstream is extracted from the baghouse breeching directly above the pilot unit. A 6-in. (~15.4-cm ID) pipe nozzle is used to extract the slipstream, and a 15-m (50-ft) run of 6-in. pipe brings the slipstream to the pilot unit flow splitter. From the flow splitter, 4-in. (~10.2-cm ID) ducts feed to both baghouses.

At the pilot unit test ports, the inlet dust loadings have varied from 0.6 to 5 g/scm (0.25 to 2 gr/scf). A typical value is about 0.7 g/scm (0.3 gr/scf). Particle size information and more detailed mass loading information are presented in Section 7.

TABLE 2. WAYNESBORO, VIRGINIA, BOILER HOUSE

Number of boilers:	4
Type:	Pulverized coal with oil cofiring capability
Capacity:	68,200, 75,000, 75,000, and 70,000 kg/hr of steam at 2860 kPa
Operation:	Continuous
Normal load:	164,000 kg steam/hr
Load variation:	(a) 143,000 kg/hr minimum to 209,000 kg/hr maximum over a year. (b) Variation up to 18,000 kg/hr within an 8-hr shift. (c) Variation up to 27,000 kg/hr within a 24-hr period.
Coal:	Highly variable Sulfur: 0.6 - 2.9 percent, average of about 1.3 percent. Ash: 6 - 27 percent, average of about 13 percent.
Emission control device:	Reverse-air baghouse

PILOT BAGHOUSES AND TEST TRAILER

A schematic of the ESFF pilot unit is provided in Figure 8. All ductwork was passed through the trailer to produce a suitable environment for test work. All ductwork downstream of the inlet flow splitter was 4-in. (~10.2-cm) Sch 40 steel pipe. The approximate locations of flow control and isolation valves are indicated in Figure 8. Testing was done through the indicated test ports which consisted of slots in the duct wall, roughly 1 cm wide by 5 cm long. A 3-in. (~7.6-cm) female pipe coupling welded to the duct (with a pipe plug) provided a gas-tight seal for each port when not in use. The ductwork was insulated with 7.6 cm (3 in.) of calcium silicate. The ports nearest the baghouses were used for all particulate testing.

Flow was measured by orifice plates on the inlet and outlet of each baghouse; a direct check of in-leakage was thus available. Flow control was by manual operation of the bypass valve and the downstream valve in each house. Blowers with a relatively flat operating curve were selected, and only slight adjustments were necessary as baghouse pressure drop changed during an operating cycle. Not shown on the schematic are the baghouse pressure drop taps, which were located just below and above the tubesheet of each baghouse. The baghouse pressure drop was continuously recorded.

Figure 9 is an isometric drawing of the ESFF pilot unit baghouses. Table 3 outlines the features of the pilot baghouses. The inlet ducts to the two baghouses are as close to identical as was possible. The two baghouses are themselves identical with the exception of the electrical hardware in the ESFF baghouse. Dirty gas enters at the bottom of the baghouse, is filtered on the outside of the bags, and returns from the top of the baghouse. Bags were installed in the baghouse from the top and the cages were then inserted into the bags. No venturis were used. The cleaning pulses issued from 0.63-cm (0.25-in.) holes drilled in the bottom of blow pipes located directly above the bag openings. The pulse energy was kept constant for all bags. Cleaning was on-line during the test programs. The cleaning pulse was of 50-ms duration from an 80-psig header. Industry standard types of diaphragm pulse valves were used, controlled by normal pulse-jet controllers.

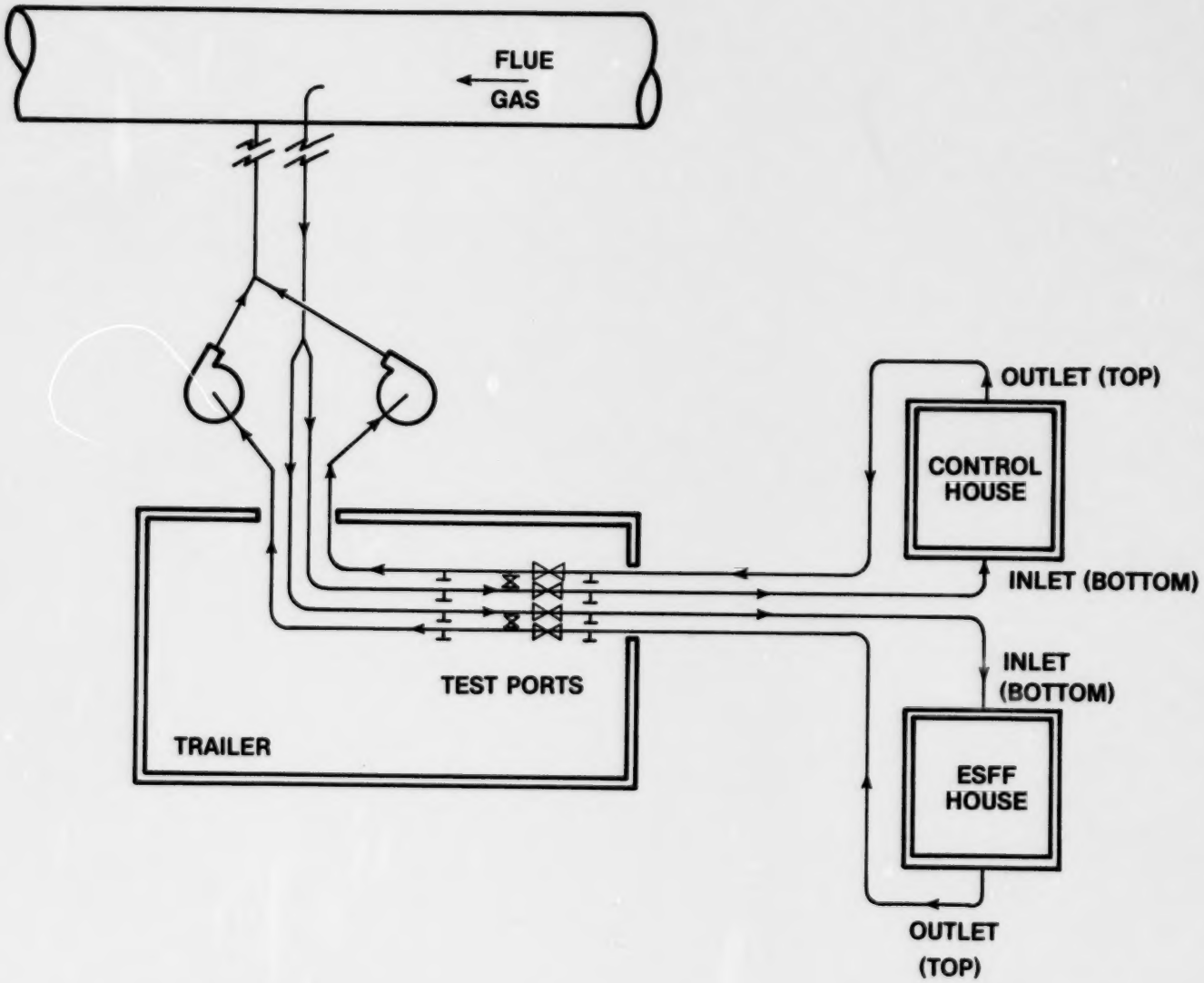

Figure 8. Schematic diagram of ESFF pulse-jet pilot unit.

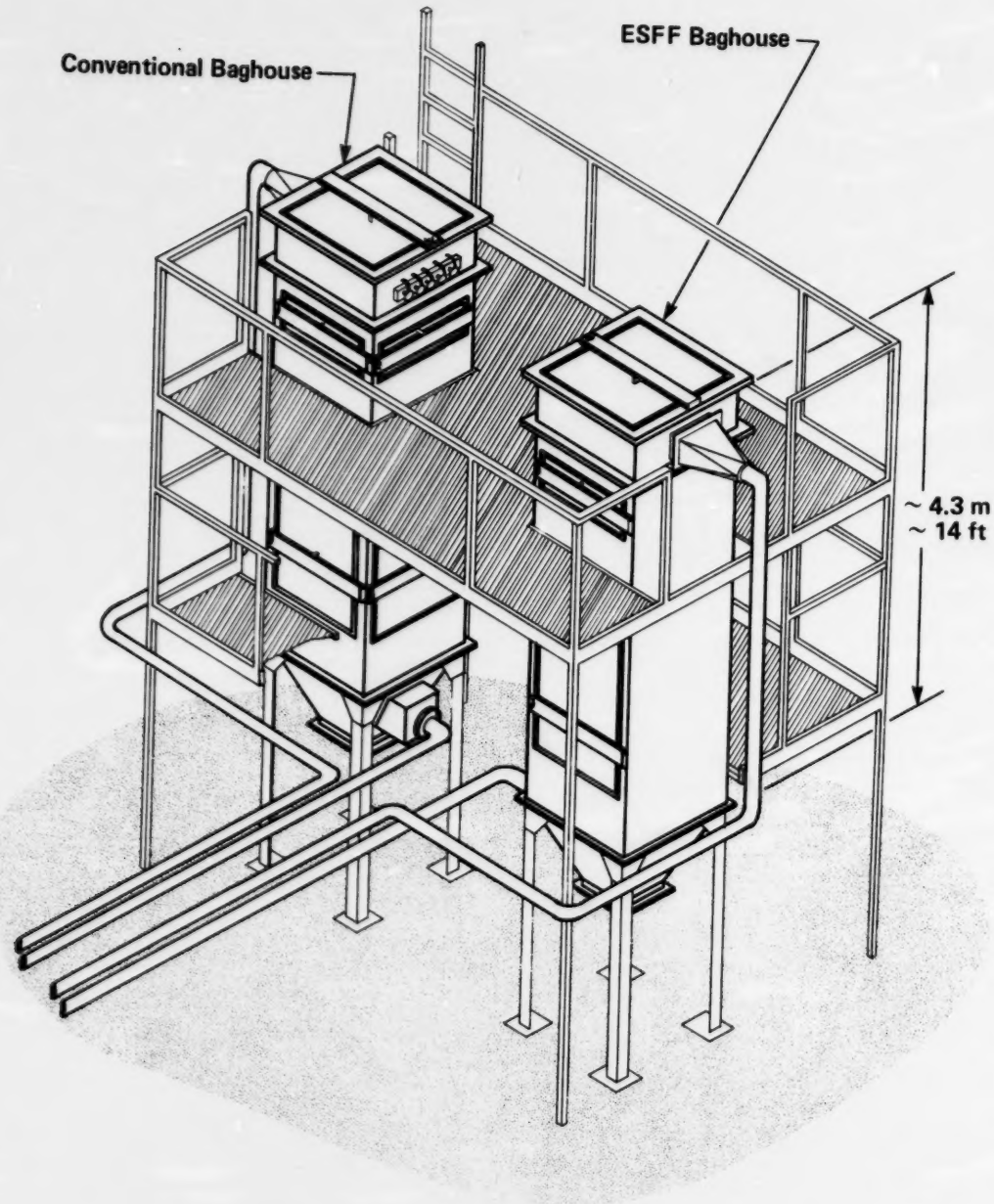

Figure 9. Isometric drawing of pilot unit baghouses.

TABLE 3. PILOT UNIT FEATURES

Basic design:	Parallel, identical pulse-jet baghouses
Baghouses:	Each 0.85 m (33 in.) square by 4.3 m (14 ft) high. Designed for 8.5 to 14.2 m^3/min (300 to 500 cfm).
	Thirteen-bag capacity; 3 rows of 3 bags, alternated with 2 rows of 2 bags; spaced 20 cm (8 in.) on centers.
	Bags are 11.4-cm (4.5-in.) diameter by 244 cm (8 ft) long. Top loading of bags.
	Insulation is 7.6 cm (3 in.) calcium silicate on ducts, 7.6 cm (3 in.) fiberglass on baghouse, additional 7.6 cm (3 in.) fiberglass over doors. All insulation is covered with aluminum sheet.
	Access doors located at 2 levels on 3 sides of the baghouses. Also top access from door on top.
	Cleaning by pulse through blow pipe located above bag. Both pressure drop and timed cleaning cycles available. A 50-msec pulse of 650 to 790 kPa (80 to 100 psia) air was used, which is typical of commercial practice.
Instrumentation:	Flow measurement by orifice, both inlet and outlet of each baghouse.
	Temperature measurement by thermometer, inlet and outlet of each baghouse.
	Baghouse pressure drop by pressure gauge and recorded via transducer.

Because of the anticipated use of the outside-harness ESFF electrode, the tubesheet holes were cut oversize at 14 cm (5.5 in.) for the 11.4-cm-diameter (4.5 in.) bag. The bag design was modified to include an enlarged cuff. The bags were sewn to be 11.4 cm (4.5 in.) in diameter over most of their 2.4-m (8-ft) length. The top 20 cm (8 in.) of each bag was expanded (through a concentric, truncated fabric cone) from 11.4 cm (4.5 in.) to 14 cm (5.5 in.) diameter to fit the oversize tubesheet hole. Top insertion of the outside-harness electrode mounted on the bag was possible. Center-to-center bag spacing was greater than that normally used on a conventional pulse jet but was the same on both baghouses. The increased spacing was needed for the outside electrodes, but the new design developed during this program and described in the following section does not appear to require additional spacing.

ELECTRICAL HARDWARE

The electrical hardware consisted of high voltage DC power supplies, current and voltage instrumentation, and the ESFF electrodes. The power supplies and instrumentation are shown schematically in Figure 10. Five identical power supply systems were provided for the ESFF baghouse. These provided flexibility in powering the ESFF electrodes and backup capability. As no more than five bags were installed during the test program, it was possible to monitor bag current and power supply current separately for each bag.

The high voltage power supplies were mounted close to the baghouse. Instrumentation and control equipment was kept at relatively low voltage for safety and was located in the test trailer.

Three high voltage electrode designs were used during the test program. The first design used was the TRI harness, as shown previously in Figure 5. The electrode wires were 0.58-mm (0.023-in.) 304 stainless steel. The connecting yarns were fiberglass. The electrodes were glued to the horizontal connecting yarns. The entire assembly was tied to the outside of the bag, and the electrical connections were made by connecting the electrodes and high voltage leads to opposite ends of bolts which were passed through the bag cuff. This outside electrode harness was used during most of the test program. Several problems were inherent in this design. The harness had the potential of restricting the bag and reducing cleaning efficiency. It was relatively fragile and difficult to install. The cage

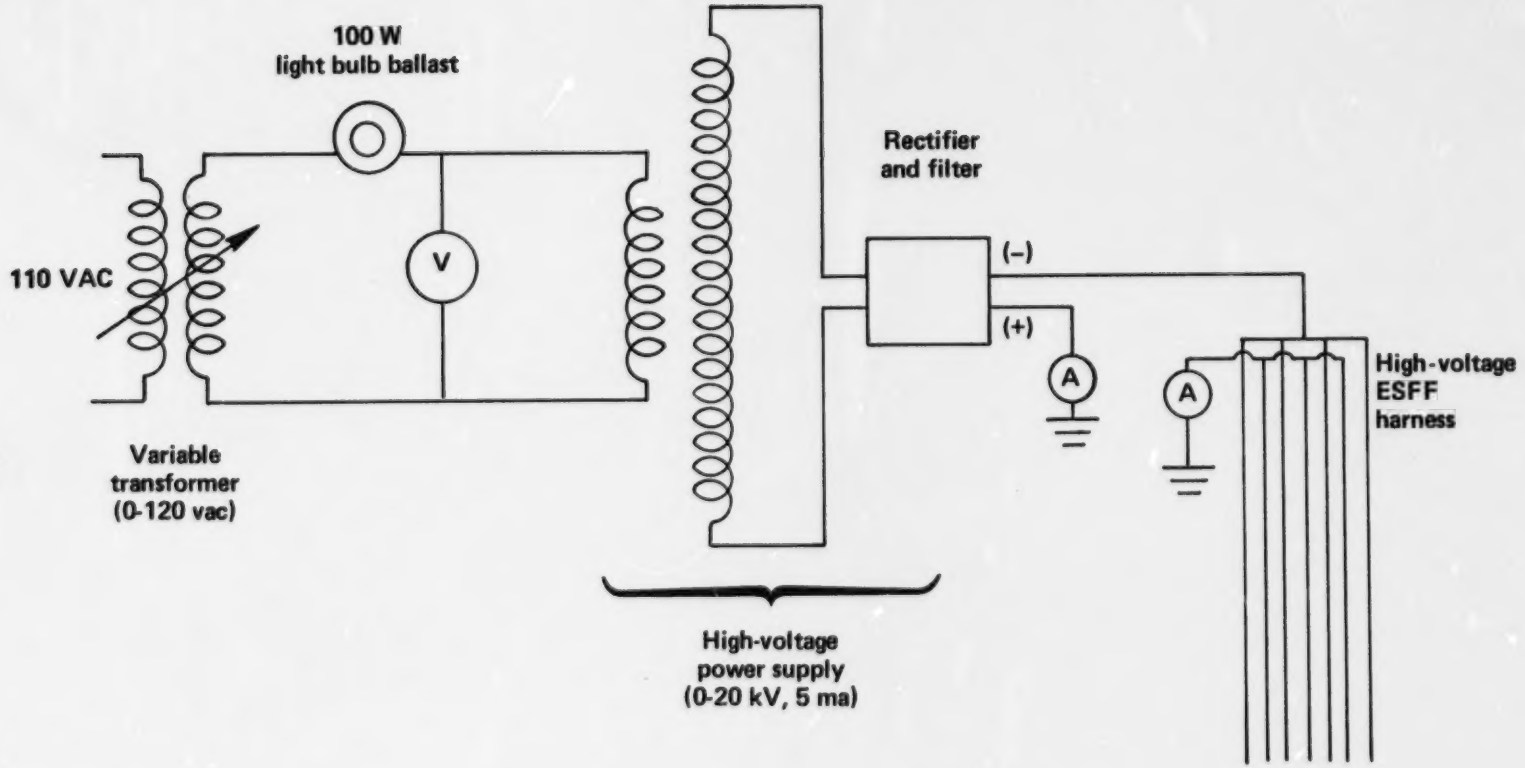

Figure 10. High voltage ESFF electrical circuit.

within the bag required coating to electrically insulate it from the harness on the outside of the bag. The harness adhesive and the baghouse cage coating were both adversely affected by the high temperature flue gas environment. In spite of these difficulties, the harnesses were used successfully during a significant portion of the test program.

The electrode design shown in Figure 11 was developed to overcome the difficulties listed above. The electrodes and cage were combined into one unit and placed inside the bag. The insulating rings were 0.64 cm (0.25 in.) thick with an outside diameter of 11.4 cm (4.5 in.) and an inner diameter of 9.5 cm (3.75 in.). The electrode spacing was 2.08 cm (0.82 in.). This configuration was not attempted initially because of laboratory data collected by TRI which indicated considerably reduced performance with the electrodes on the clean side of the fabric. As is reported in Section 7, the pilot unit results were more favorable than the laboratory results; the inside cage worked as well as the harness did but without the inherent problems. A second design of an inside harness was also built and used at the pilot unit (Figure 12). The vertical 0.32-cm (0.125-in.) wires, alternately charged, were again used for electrodes. Added strength was provided by the steel inner rings; electrical insulation was provided by slip-on Teflon® tubing. Sixteen equally spaced wires were used, resulting in a surface-to-surface electrode spacing of 1.93 cm (0.76 in.).

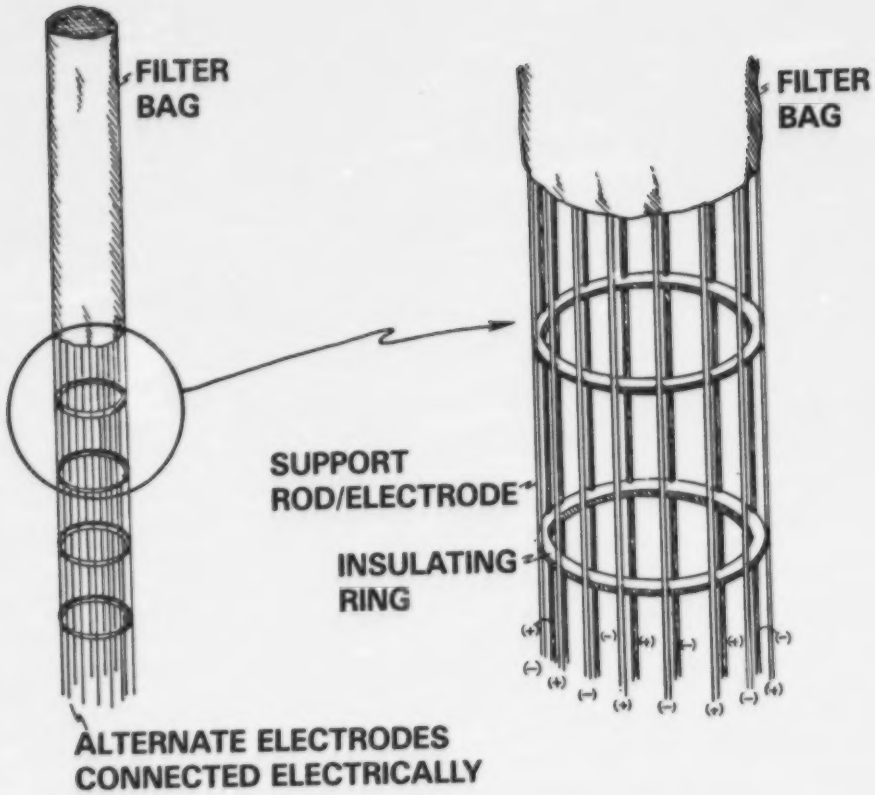

Figure 11. Inside electrodes utilizing insulating ring spacers.

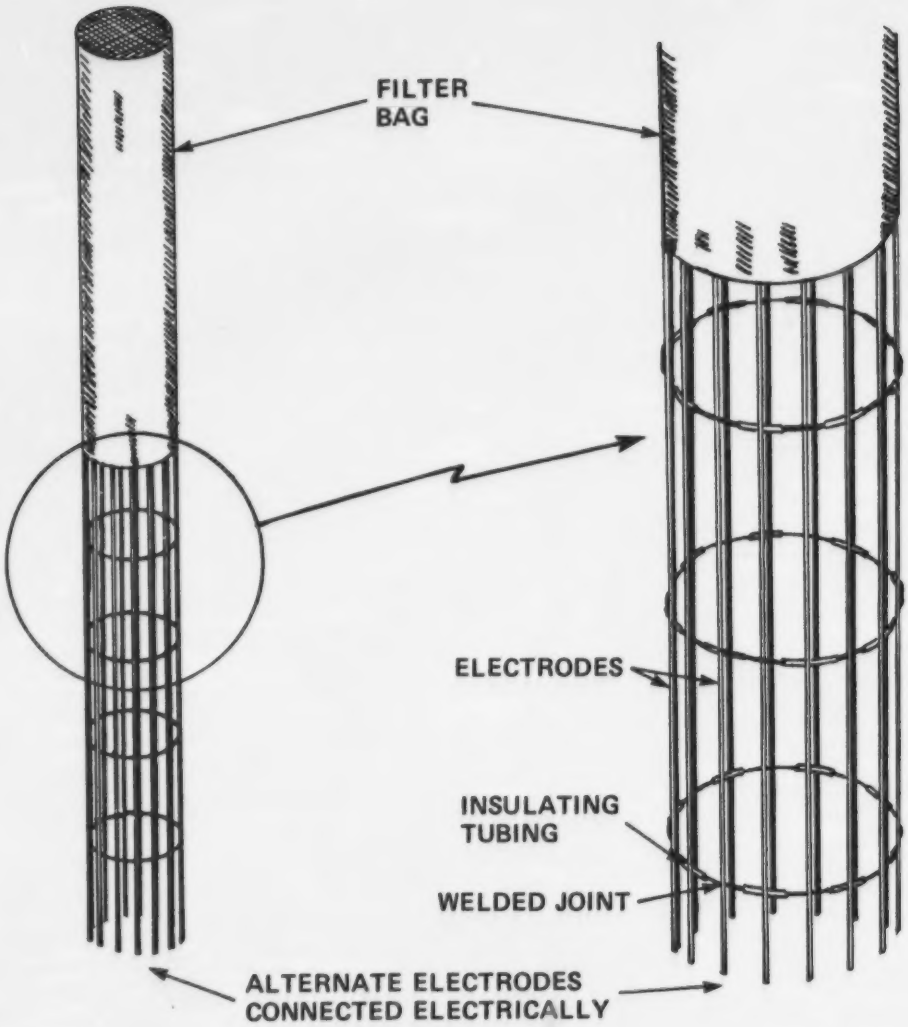

Figure 12. Inside electrodes utilizing insulating tubing on cage rings.

SECTION 6

OPERATION

INTRODUCTION

The field operation of the pilot unit consisted of a break-in or check-out phase followed by a test program to determine the operational characteristics of the ESFF baghouse. The initial goal of the test program was to simply demonstrate that the ESFF effect would occur in the field environment. Once this crucial point was demonstrated, a parametric study of the ESFF effect was initiated. The test program, outlined in Table 4, is discussed below as a chronological series of test periods. Electrical and other hardware problems which developed during the early test periods forced a steady evolution in equipment design, and it was necessary at times to repeat earlier test series with the new equipment. The results of all test series have been collected and are presented in Section 7.

BREAK-IN PERIOD--MODIFICATIONS

Parallel Test Validation

To obtain reliable comparisons between the ESFF and control baghouse, the initial test program was directed to verifying that the two baghouses did, in fact, have identical inlet conditions. Each baghouse was equipped with five Teflon® felt bags (no electrical enhancement), and the flow through each baghouse was set at the same rate. Throughout the entire test program, cleaning was on-line utilizing a 50-ms pulse of cleaning air. Proof of satisfactory inlet conditions was then obtained by comparing the bag pressure drop for each baghouse. The pressure drops were found to remain well within 10 percent of each other. Inlet mass loading tests also agreed when run simultaneously; considerable variation with time was evident.

TABLE 4. SUMMARY OF ESFF PULSE-JET PILOT UNIT TEST PROGRAM

Test series	Time period	Purpose	Highlights
Break-in	May 1-June 15, 1980	Check out hardware and demonstrate that the parallel baghouses had identical inlet conditions.	Hardware problems corrected; inlets essentially identical.
1	June 15-July 18, 1980	Demonstrate that ESFF effect is present at pilot unit and begin parametric study.	ESFF effect present. Hardware shortcomings were evident.
2	July 24-August 8, 1980	Parametric test of ESFF as function of field, cleaning cycle, and face velocity.	Successful test program with some difficulty with ESFF hardware.
3	September-December 1980	Parametric test with improved electrodes, new fabrics.	Inside electrodes functioned well; test results similar to Test Series No. 2. Ability to operate at high face velocity demonstrated.
4	January-February 1981	Longer term testing at high face velocities.	Successful operation at 3- and 4-cm/s (6- and 8-ft/min) face velocities.

Ambient Air In-Leakage

Leakage of ambient air into the pilot units between inlet and outlet test ports was of major concern as it affected the flue gas conditions and actual filtering velocity through the bags. If the comparison of the two collectors was to be valid, any inward leakage had to be known and reduced to acceptable levels in both collectors.

The fact that testing was to be conducted using only three to five bags and a low gas volume made any leakage more significant. The baghouse design, with seven inspection doors in each baghouse, made the task more difficult.

Door Leakage

Each baghouse is equipped with seven doors for inspection and bag installation. The original design used a knife edge against a Teflon® felt pad as the principal seal. This did not prove to be adequate for the leakage levels required.

Adequate sealing (<10 percent leakage) was obtained by the addition of silicone rubber gasketing at all door sealing edges. It was recognized that the silicone rubber would deteriorate slowly in the sulfur dioxide environment; hence, the gaskets were monitored and periodic replacement was necessary. Adequate sealing was maintained throughout the test program.

Hopper Leakage

The ash hoppers are equipped with dual sliding gate valves with the intention of providing on-line ash dumping capability. Air leakage through the valves was found to be excessive both for testing purposes and for dumping. A 57-L (2-ft^3) air-tight box was arranged under each hopper. This box was emptied once each day.

Heat Losses

Significant problems were initially encountered with excessive heat loss from the ductwork and baghouses. The resultant temperature drop resulted in occasional operation of the baghouses, piping, and fans at below the acid dew point. This was of particular concern since it was probable that acid condensation on the bags would provide an electrical current path. The original

design included 7.6 cm (3 in.) of insulation on all ducts and the baghouse walls; however, typical operation resulted in a baghouse outlet temperature of 80° C and an inlet temperature of 160° C. Direct heat effects were due to in-leakage and heat loss across the insulation, and the problem was made worse by a relatively low flow (five bags). The acid dew point was expected to be between 120° and 130° C.

This low temperature problem was corrected by several modifications. Through very careful monitoring of air in-leakage, excessive leaks were located and corrected. The large doors on three sides of each baghouse were not insulated as well as was the main body of the baghouses and were suspected of being a major heat loss area. This proved to be the case, and additional insulation was provided over these doors. The third step taken was the installation of heaters, rated at 8000 W, in each baghouse. These heaters were mounted inside the access doors and provided the required supplemental heating. This combination of measures has proven to be satisfactory, and no further acid condensation was observed.

Gas Flow Measurement

The flue gas flow was set up initially by pitot tube measurement each day. In addition, each baghouse was equipped with both an inlet and outlet gas flow orifice. The orifices were used as the normal flow rate measurement instrument, with the pitot measurement used as a check.

The gas flow measurement orifices were calibrated against a pitot tube. This calibration showed all orifices to be within 10 percent of the expected calculated values. During subsequent testing, erratic operation was noted; this was corrected by daily purging the orifice sensing lines of dust using compressed air. The calibrations were repeated, and an orifice coefficient was determined for each orifice.

Bag Conditioning

The start-up bags were removed and four new napped Teflon® felt bags were installed in each baghouse on June 18th. This fabric was a 23-oz felt (Du Pont Armalon XT-2363) made by needling fiber to both sides of a scrim fabric. The fabric has the following specifications:

Weight, oz/yd^2	23	(780 g/m^2)
Tensile strength, 2-in. (5-cm) strip, lb	180x150	(801x667 N)
Mullen burst, psi	250	(1723 kPa)
Thickness, in.	0.05	(1.3 mm)
Frazier porosity, cfm/ft^2 @ 0.5 in. H_2O	15-65	(7.6-33 cm/s @ 0.125 kPa)

Measurements of the porosity of the actual fabric used averaged 23 cfm/ft^2 (11.7 cm/s) at 21° C (70° F); this decreased to 6.5 cfm/ft^2 (3.3 cm/s) corrected to 21° C (70° F) at an air temperature of 205° C (400° F). New electrical harnesses were installed on the bags in the ESFF baghouse. The bag break-in sequence is described below:

1. The new bags were started up on ambient air at a face velocity of 1 cm/s (2 ft/min) with the heaters on. The system was on bypass with no flue gas. The outlet temperature rose to 65° C (150° F) in 2.5 hours and was up to 80° C (175° F) the following morning.

2. All the ESFF bags were set to 4 kV/cm. Note: From this time on, the electrical field was kept on the ESFF bags at all times.

3. Both baghouses were placed on-stream at a face velocity of 1 cm/s (2 ft/min) and held until a pressure drop of 0.25 kPa 1 in. w.c. built up. This period was planned to "condition" the new bags.

INITIAL TEST SERIES: MID-JUNE THROUGH MID-JULY 1980

The test program began with a test series utilizing the napped Teflon® felt bags, which had been conditioned, and the outside harness electrode. This test series confirmed that the ESFF effect was present at the pilot unit. Pressure drop ratios (PDR) of 0.33 to 1.2 were recorded during this test period. Unfortunately, several problems occurred which reduce the usefulness of the data. One electrode harness failed, and the failure was not discovered until the end of this series. Thus, one of the four bags ceased to be an ESFF bag at an unknown point in time, leading to distortion of the PDR results. In addition, the voltage record was found to be incorrect due to instrumentation error. These data were not analyzed further, but it was clear that the ESFF effect was present, and several design improvements were made based on experience gained.

SECOND TEST SERIES

Based on observations of the initial test series and following correction of the electrical problems, another series of tests was run between July 24 and August 8, 1980. During this test series, the face velocity was maintained at 3 cm/s (6 ft/min), and the field voltage remained stable up to 4 kV/cm. Testing was limited to 4 kV/cm and below due to cage insulation limitations. In-leakage was constantly checked. To nullify the small differences in ambient air leakage, equal inlet gas flows were maintained during the test cycle to insure equal dust loading, and equal outlet gas flows were maintained during all pressure drop readings to insure equal face velocities at time of reading.

The objectives of this test series were to:

1. Generate PDR versus field strength data and compare to TRI results.
2. Define the pressure drop versus time curve over 15- to 30-min cycles.
3. Define the residual pressure drop stability with time.
4. Obtain as much bag on-line time as possible.
5. Define mass and particle size distributions and efficiencies.

The entire test series utilized outside electrode harnesses and insulated cages. The results are reported in Section 7. The test series was terminated to allow the construction of new insulated cages to use with outside electrodes and the construction of the inside electrode assemblies.

THIRD TEST SERIES

The third test series was run from September through December 1980. This test series utilized both the outside harness and the inside electrodes and three different fabrics. The electrode assemblies used were:

1. The outside harness as shown in Figure 5.
2. The 15-wire inside harness as shown in Figure 11.
3. The 16-wire inside harness as shown in Figure 12.

In addition to the 23-oz napped Teflon® felt described above, a woven glass fabric and a novel single-sided Teflon® felt were used during this test series.

The fiberglass bags used during this test series were made from J. P. Stevens 648-45 woven fabric, which utilized a texturized or bulked fill yarn and a 10-percent Teflon® B finish. The specifications of this fabric are reported below:

Weight, oz/yd^2	16.8	(570 g/m^2)
Permeability, cfm/ft^2 @ 0.5 in. H_2O	35-55	(18-28 cm/s @ 0.125 kPa)

	Warp		Fill	
Tensile strength, lb/in.^{2} (kPa)	200	(1380)	100	(690)
Count, threads/in. (threads/cm)	50	(≃20)	30	(≃12)
Yarn	37	1/0	75	1/3 texturized

A new, experimental felt was also tested. This 17-oz single-sided felt is designated Armalon E9223-20 by Du Pont. This fabric is needled to only one side of the scrim fabric. The E9223-20 properties as reported by Du Pont are as follows:

Weight, oz/yd^2	16.6	(563 g/m^2)
Tensile strength, 2-in. (5-cm) strip, lb	100x120	(445x534 N)
Mullen burst, psi	180	(1240 kPa)
Thickness, in.	0.047	(1.2 mm)
Frazier porosity, cfm/ft^2 @ 0.5 in. H_2O	58	(29.6 cm/s @ 0.125 kPa)

The test conditions are summarized in Table 5 for the four test periods which comprise the third test series. The September test runs were the last with the outside harness configuration. The problems described in Section 5 (Electrical Hardware) had become relatively serious, and considerable maintenance was required to obtain reliable data. Experience with electrodes is described in more detail below.

The inside electrode configuration was installed for the next test period (October 3-27, 1980). A wide range of operating conditions was investigated to evaluate the inside electrode with the 23-oz Teflon® felt.

TABLE 5. THIRD TEST SERIES OPERATING CONDITIONS

Date	9/15/80-9/30/80	10/3/80-10/27/80	11/10/80-11/20/80	11/21/80-12/12/80
Fabric	23-oz Teflon® felt	23-oz Teflon® felt	17-oz Woven glass	17-oz Teflon® felt
Electrodes	Outside harness	15-Wire inside	16-Wire inside	16-Wire inside
Field strength	⩽ 3.8 kV/cm	⩽ 4.6 kV/cm	⩽ 3.0 kV/cm	⩽ 4.9 kV/cm
Face velocity	2-4 cm/s	1.5-4 cm/s	1.5-3 cm/s	2-3 cm/s
Cleaning intervals	12 and 15 min	5, 10, 12, and 15 min	30 min	10 and 30 min
Number of bags per baghouse	4	2-4	4	4

The woven glass fabric was evaluated for a short period in November 1980. During the check-out and break-in phase of the test, severe electrical shorts developed from the electrodes to the bag surface, resulting in holes in the bags. The surface of the bag appeared to have become conductive for some reason, allowing the shorts to take place. Boiler records did not indicate anything unusual, and the temperatures remained about normal. The bags were replaced and the test continued at lower voltages. The results were not as impressive as those obtained with the Teflon® felt bags (Section 7).

The limited success of the woven glass bags and inability to operate at high fields led to a decision to change to the lighter weight Teflon® felt bags. This test series was run November 21 through December 12, 1980. Results are compiled in Section 7.

FOURTH TEST SERIES

The final pulse-jet baghouse test series was run during January and February 1981. The purpose of the test series was to evaluate operation of the ESFF baghouse at increased face velocities. Pressure drop and particulate removal were both monitored. During this test, both baghouses were equipped with the 17-oz Teflon® felt bags. The inside electrodes were used. The control baghouse was operated at a face velocity of 2 cm/s (4 ft/min) throughout the test period. Conditions in the ESFF baghouse were varied from 2 to 5 cm/s (4 to 10 ft/min) face velocity at various cleaning intervals. The field was (with one exception) kept at 4 kV/cm. The test series operating pattern is summarized in Table 6.

EXPERIENCE WITH ELECTRICAL HARDWARE

The power supplies and instrumentation described in Section 5 (Electrical Hardware) functioned well throughout the test program. Power requirements were relatively low at 50 to 100 μA per power supply through most of the test program.

The electrodes, on the other hand, did present some problems. The outside harness electrodes (Figure 5) were used initially. The initial problem encountered was a slight misalignment of the electrode wires and some tendency for the wires to curl toward a neighboring wire. Sparking developed, eventually leading to shorts and continuous high currents. This problem was

TABLE 6. HISTORY OF FOURTH TEST SERIES

Date		Face velocity		Clean interval	Field	Test duration
Start	Stop	(cm/s)	(ft/min)	(min)	(kV/cm)	(hr)
1/6	1/12	3	6	30	5	143
1/12	1/13	1.5	3	30	4	19
1/13	1/14	2	4	30	4	28
1/14	1/16	4	8	15	4	45
1/16	1/19	3	6	30	4	72
1/19	1/26	4	8	15	4	168
1/26	1/28	5	10	10	4	46
1/28	1/29	4	8	10	4	23
1/29	2/2	5	10	10	4	97
2/2	2/4	2	4	30	4	48
2/4	2/5	3	6	30	4	16
2/5	2/5	2	4	30	4	3

corrected with more careful construction of the harness and the use of slip-on Teflon® insulating tubing near the top and bottom of the harness.

After about 2 months of exposure to the flue gas environment, the materials used in the harness construction and cage coating were noticeably deteriorated. The elastomeric adhesive used to construct the harness had become brittle. The silicone resin-based conformal coating used to insulate the cages also became brittle and developed cracks. Sparking and electrical shorts became a regular occurrence. The cage coating was particularly troublesome.

The new inside electrodes/cage combination was installed in October 1980 and significantly improved operation. The initial inside electrode design with Teflon® ring spaces (Figure 11) functioned very well electrically, making it possible to operate at 5 kV/cm. The Teflon® rings appeared to reduce cleaning efficiency, however, presumably because the rings broke up the cleaning pulse wave front. In addition, the rings were weak structurally, and most failed when tested with 2.5 kPa (10 in. H_2O) of bag pressure drop. The second inside cage design (Figure 12) was intended to provide added strength and better cleaning. These goals appear to have been met; however, there was some reduction in electrical capability. The Teflon® tubing insulation failed electrically occasionally, due to a combination of physical distortion and electrical stress.

SECTION 7

RESULTS

INTRODUCTION

The physical effect of electrostatic augmentation of fabric filtration is to modify the microstructure of the collected dust cake. Changes in the appearance of the dust cake can sometimes be detected, but the primary measure of the ESFF effect has been the reduction of pressure drop at various baghouse operating conditions. The sections below address various aspects of the ESFF effect. The ESFF effect most clearly evident at the pilot unit was a decrease in the slope of the pressure drop versus time plot. At constant dust loading, this slope is a measure of specific dust cake resistance. Unless otherwise indicated, the statement in the following sections about the presence of the ESFF effect refers to the fact that the slope of the pressure drop curve was less for the ESFF baghouse than for the control baghouse.

DUST CAKE

Visual Observations

The dust cake collected by the ESFF baghouse appeared visually to be nearly identical with that collected by the control baghouse. The dust cake in the immediate vicinity of the electrodes seemed slightly thinner in some observations, but the difference was largely subjective and may have been due to the physical presence of the electrodes and cage rather than the cake structure. The dust cake did not cover the outside electrodes even when very thick; the electrodes cut through the dust cake during the cleaning process. The outside electrodes did become partially coated with dust to about twice their diameter in some places. This deposit consisted of both clean and thickly coated regions. No interference with the ESFF effect was detected.

Some electrode designs restricted uniform cleaning of the bags as evidenced by a thick dust cake on the lower half of the bag. This was true of the outside harness (bag motion restrained) and of the inside electrode design using Teflon® ring insulators (rings breaking up pulse shock wave). The effect of this condition on our results was not obvious. Much of the pilot plant data were taken using these electrode configurations; the inside electrodes which allowed complete cleaning did not produce a significantly greater ESFF effect than did the outside electrodes.

Effect of Dust Cake Thickness

TRI bench-scale test work, which indicated that the position of the electrodes with respect to the fabric surface was critical, led to an expectation that dust cake thickness might be important in an ESFF baghouse. Early in the test program an attempt was made to operate for extended periods (1½ to 2 hours without cleaning) and to build up an unusually thick dust cake. Only in one instance was an apparent reduction in the ESFF effect observed. Dust cake thickness did not appear to be important at normal operating conditions. The ESFF effect was observed to continue with a dust cake of 2- to 3-mm thickness, which is several times the outside electrode diameter. Later operation with the inside electrodes further reduced concern about electrode position and dust cake thickness.

Dust Density

The bulk density of the collected baghouse dust was measured by weighing the partially filled baghouse hoppers and gauging the volume of the collected dust. The results of this experiment are presented in Table 7.

The average bulk density of the ESFF fly ash, at 0.23 g/cm^3, is 80 percent of the average bulk density of fly ash collected in the conventional baghouse.

Fly Ash Resistivity

The resistivity of the dust layer is important because the high voltage electrodes are in direct contact with the dust cake and fabric. Low resistivity would cause high currents and, in an extreme case, lead to electrical shorts. The resistivity of a fly ash sample was determined in the

TABLE 7. BULK DENSITY OF COLLECTED FLY ASH

Date of measurement (1981)	ESFF dust density (g/cm^3)	Conventional dust density (g/cm^3)
9/19	0.17	0.23
9/24	0.16	0.18
9/30	0.23	0.26
10/9	0.23	0.30
10/13	0.23	0.21
10/14	0.27	0.29
10/15	0.31	0.37
10/16	0.25	0.31
Average	0.23	0.27
Standard deviation	0.05	0.06

laboratory by Southern Research Institute with no sulfur oxides present. The resistivity of the ash for 3 and 6 ppm SO_3 was then calculated using the techniques presented by Bickelhaupt.[20] The results are presented in Figure 13. These data show that the performance of the ESFF baghouse could be very sensitive to temperature due to the sensitivity of resistivity to temperature. Normal baghouse operating temperature is between 150° and 160° C, but at low flow rates on cold days the temperature has dropped to the 120° C region. This is near the acid dew point for some of the coals burned at Waynesboro; even without condensed acid the resistivity at 120° C is more than an order of magnitude less than it is at 150° C.

Fly Ash Charge

The charge-to-mass ratio was measured for the pilot unit fly ash. The results are presented in Table 8. An extractive sampling technique, as described in Appendix B, was used. The charge averaged a negative 0.49 μC/g with a standard deviation of 0.28 μC/g. This value is similar to that measured at another coal-fired industrial boiler.[21]

DUST CAKE FLOW RESISTANCE

The ESFF effect can be easily seen in a plot of baghouse pressure drop versus time. Figure 14 is an example. The pressure drop of the ESFF baghouse does not increase as rapidly as does that of the conventional baghouse. As the same amount of dust is being deposited on the bags in both baghouses, the difference must be in the resistance of the dust cake to flow. PDR, as defined earlier, is a measure of the relative magnitude of this change. The difference in residual pressure drop will be discussed in a later section.

Figure 15 presents PDR data as a function of electric field strength for three fabrics at three operating conditions, all except the TRI data utilizing the inside cage. The smoothed curve obtained by TRI from data for 23-oz Teflon® fabric is included for comparison. The data for both Teflon® fabrics and for the glass fiber fabric fall in roughly parallel bands. The data for the outside electrode harness on Teflon® fabric fall along the Teflon® fabric line, indicating no significant difference due to the electrode type. PDR was not as strong a function of field strength at the pilot

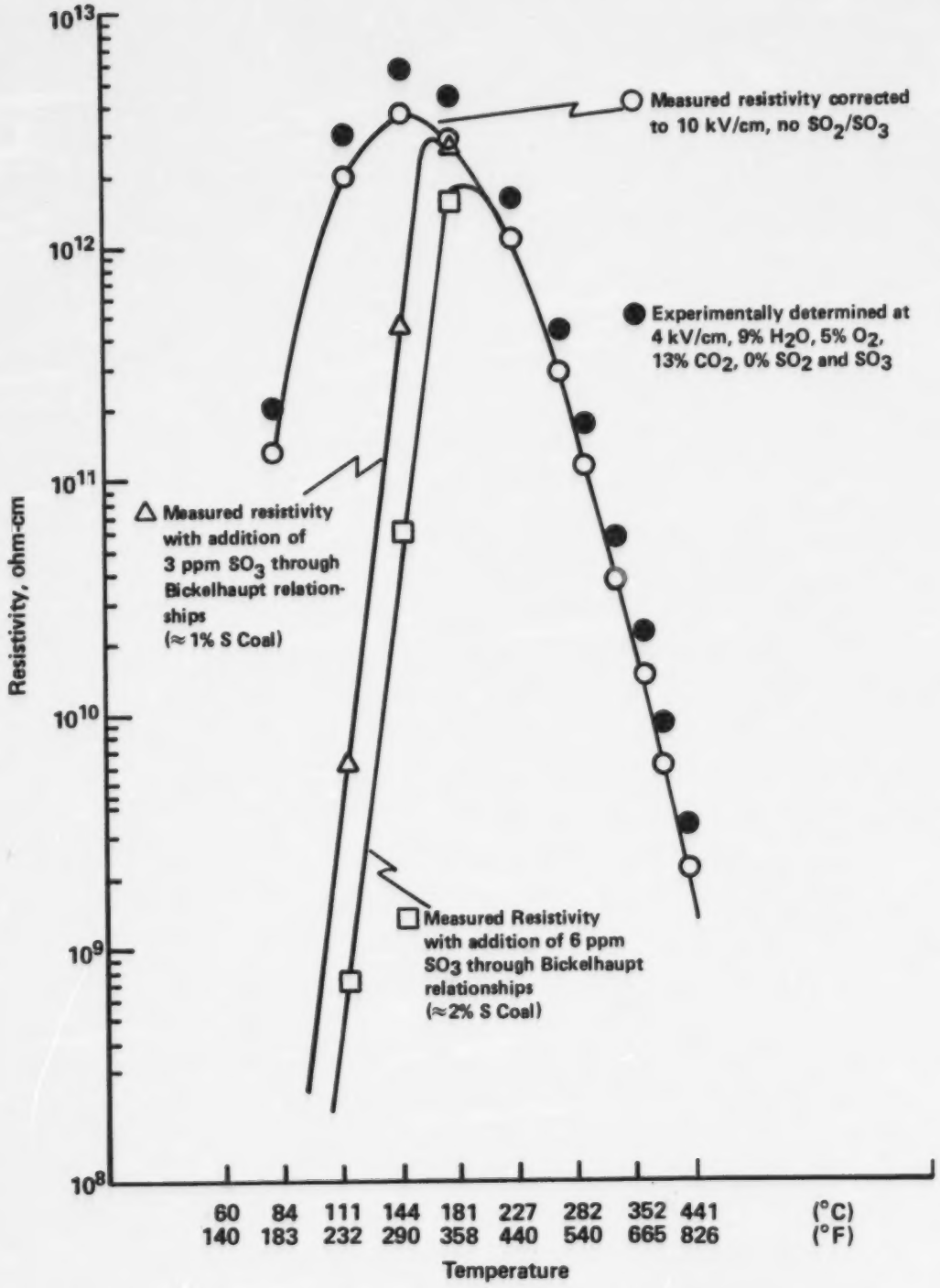
Resistivity, ohm-cm
10^{13}
10^{12}
10^{11}
10^{10}
10^{9}
10^{8}
Measured resistivity corrected to 10 kV/cm, no SO_2/SO_3
Experimentally determined at 4 kV/cm, 9% H_2O, 5% O_2, 13% CO_2, 0% SO_2 and SO_3
Measured resistivity with addition of 3 ppm SO_3 through Bickelhaupt relationships (≈ 1% S Coal)
Measured Resistivity with addition of 6 ppm SO_3 through Bickelhaupt relationships (≈2% S Coal)
60 84 111 144 181 227 282 352 441 (°C)
140 183 232 290 358 440 540 665 826 (°F)
Temperature

Figure 13. Waynesboro fly ash resistivity (point-to-plane breakdown).

TABLE 8. PARTICULATE CHARGE-TO-MASS RATIO

Run no.	Date	Time	Charge-to-mass (μC/g)
	6/18/80	1622	0.45
3	10/23/80	1345	0.40
5	10/23/80	1510	0.46
6	10/23/80	1549	2.35[a]
7	10/23/80	1625	0.52
8	10/24/80	0829	0.26
10	10/24/80	0920	0.42
11	10/24/80	0939	1.24
12	10/24/80	1010	0.31
	Mean		0.49
	Standard deviation		0.28

[a] Not included in average.

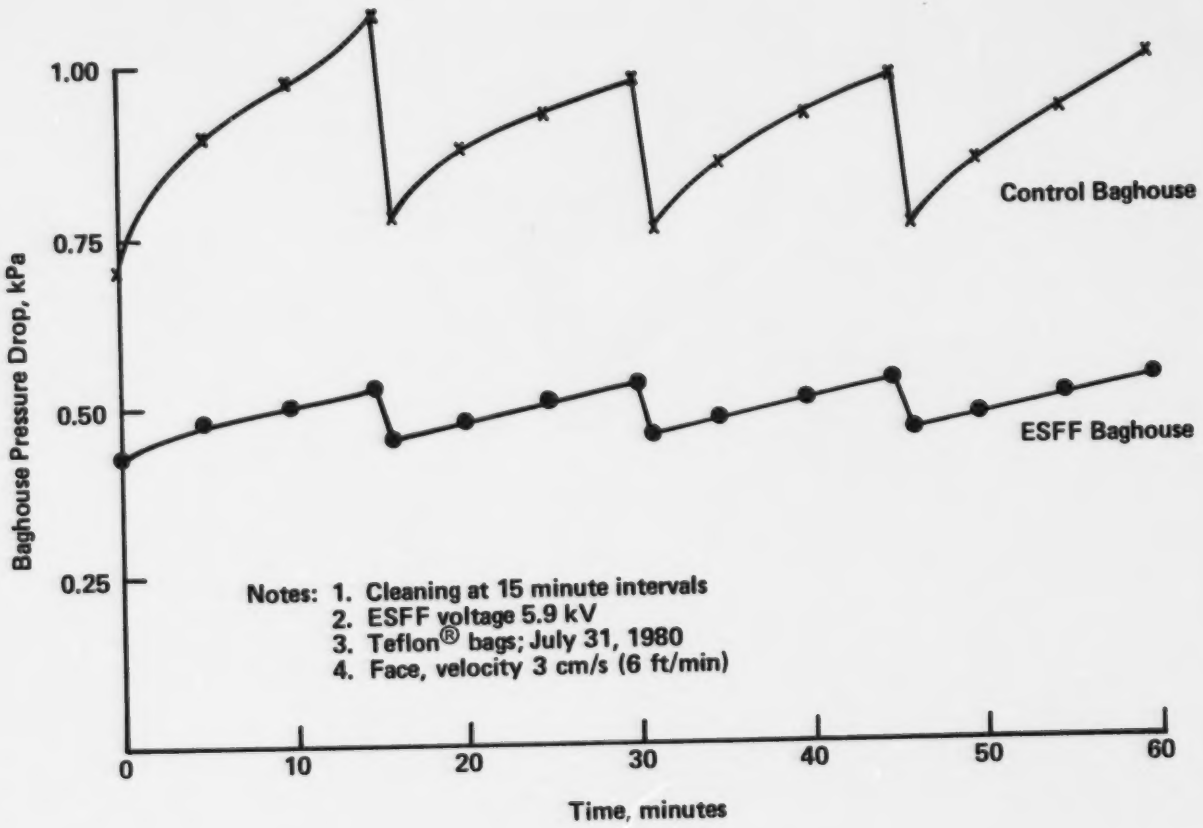

Figure 14. Pressure drop plot for pilot baghouse.

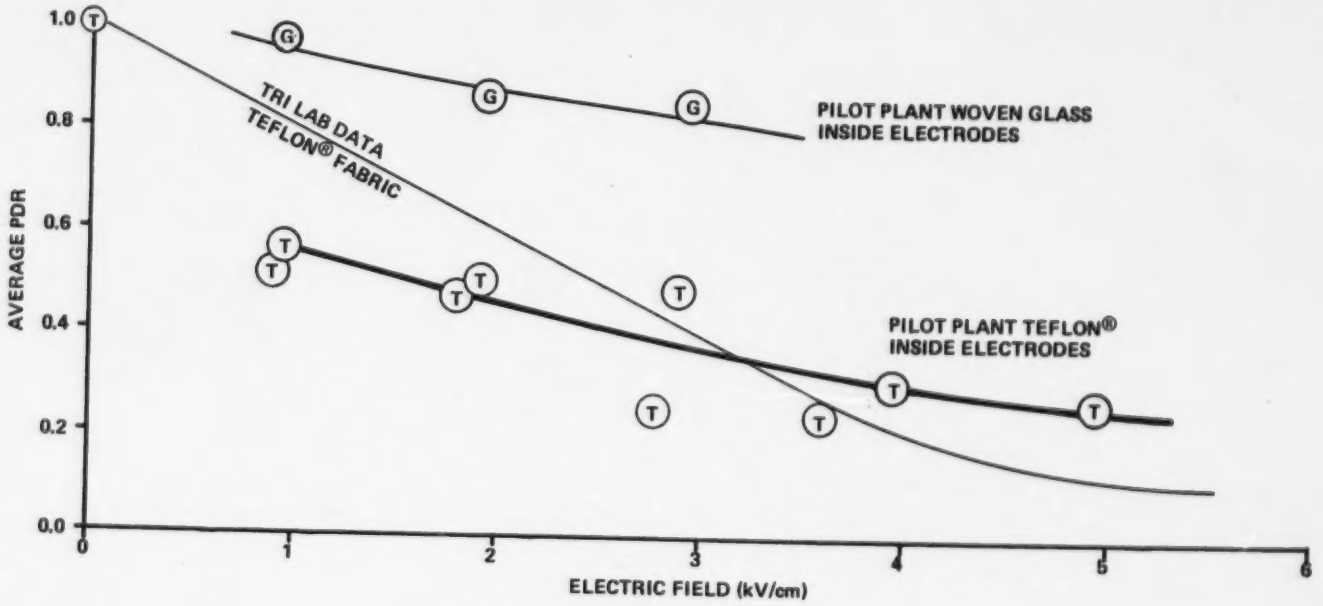

Figure 15. PDR-field strength relationship for Teflon® and glass fabrics.

unit as was the case for the TRI bench-scale equipment. As the operating conditions were very different, lack of agreement is not surprising. The two Teflon® fabrics do not have significantly different PDR-field strength relationships.

PDR is apparently not affected by face velocity. Figure 16 presents PDR data at various face velocities with field strength as a parameter for Teflon® fabric. There is no trend in PDR as face velocity changes. The insensitivity of PDR to field strength at high fields is also evident in this figure.

REDUCED RESIDUAL PRESSURE DROP

ESFF has a significant effect on the residual pressure drop of the fabric. Figure 17 is a plot of residual pressure drop for both baghouses over a 5-day period. The ESFF baghouse was in stable operation at about 0.5 kPa (2 in. H_2O), while the conventional baghouse had risen above 1.5 kPa (6 in. H_2O) pressure drop and was still rising. This effect was consistently encountered. It was possible through repeated multiple-pulse off-line cleaning to return both baghouses to about the same pressure drop. The difference in residual pressure drop soon developed again. The amount of scatter in the data coupled with the limited range of parameter variation prevented any correlation with field strength, face velocity, or cleaning cycle duration. The average reduction in residual pressure drop, expressed as:

$$R = \frac{\Delta P_{control} - \Delta P_{ESFF}}{\Delta P_{control}} \qquad (8)$$

where ΔP = residual pressure drop, was 0.42, with a standard deviation of 0.27 (data for September and October 1980 with 23-oz Teflon® fabric at various operating conditions).

OPERATION AT INCREASED FACE VELOCITY

The ability of the ESFF baghouse to operate at a lower residual pressure drop suggested that it might be possible to operate at an increased face velocity without blinding. Figure 18 presents several hours of pressure drop data for both baghouses at 2.5 cm/s (5 ft/min) and at 4 cm/s (8 ft/min). The superior performance of the ESFF baghouse is evident.

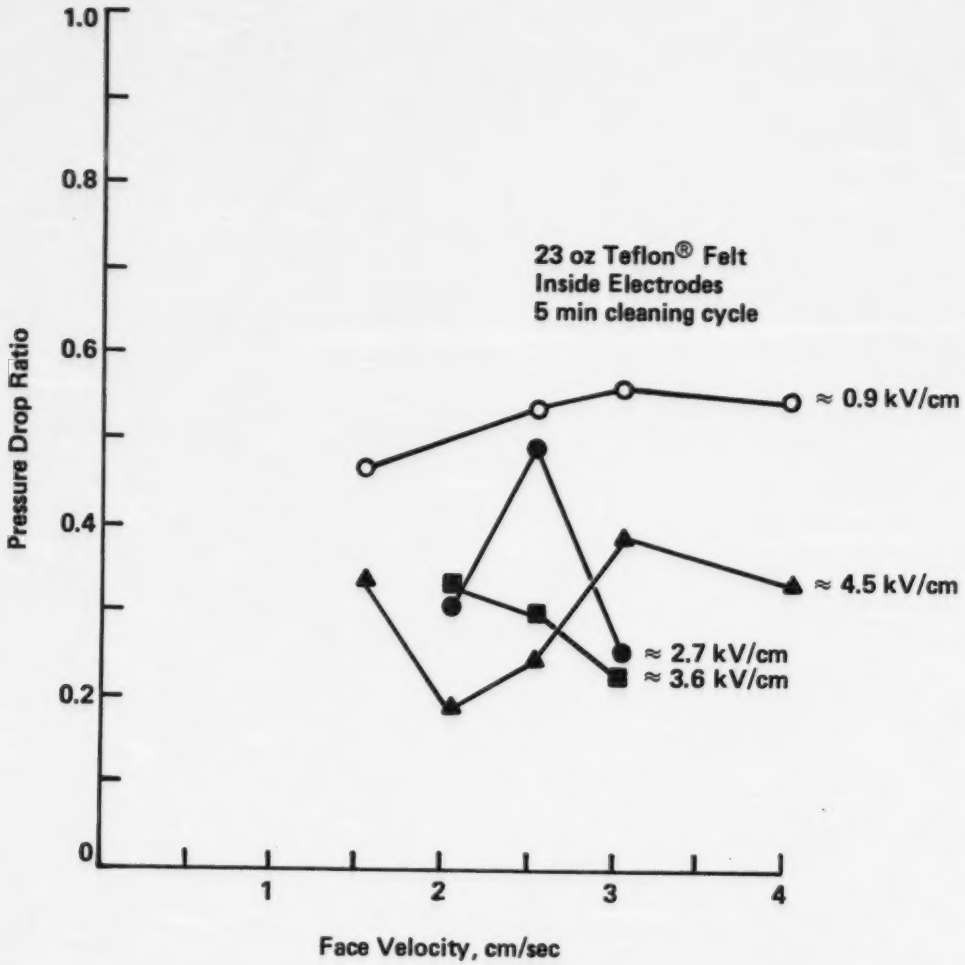

Figure 16. Pressure drop ratio as a function of field strength and face velocity.

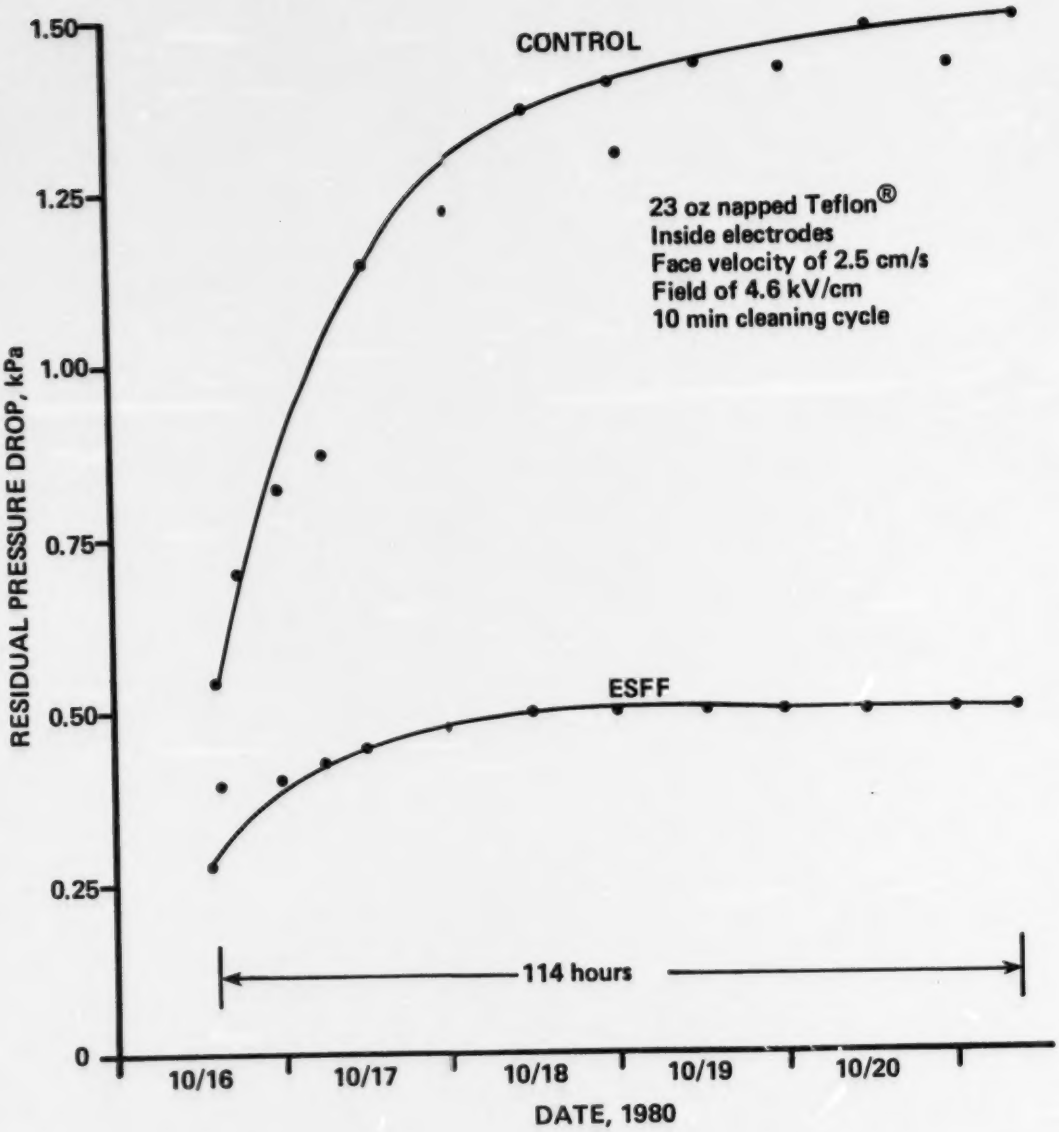

Figure 17. Residual pressure drop for ESFF and control baghouses.

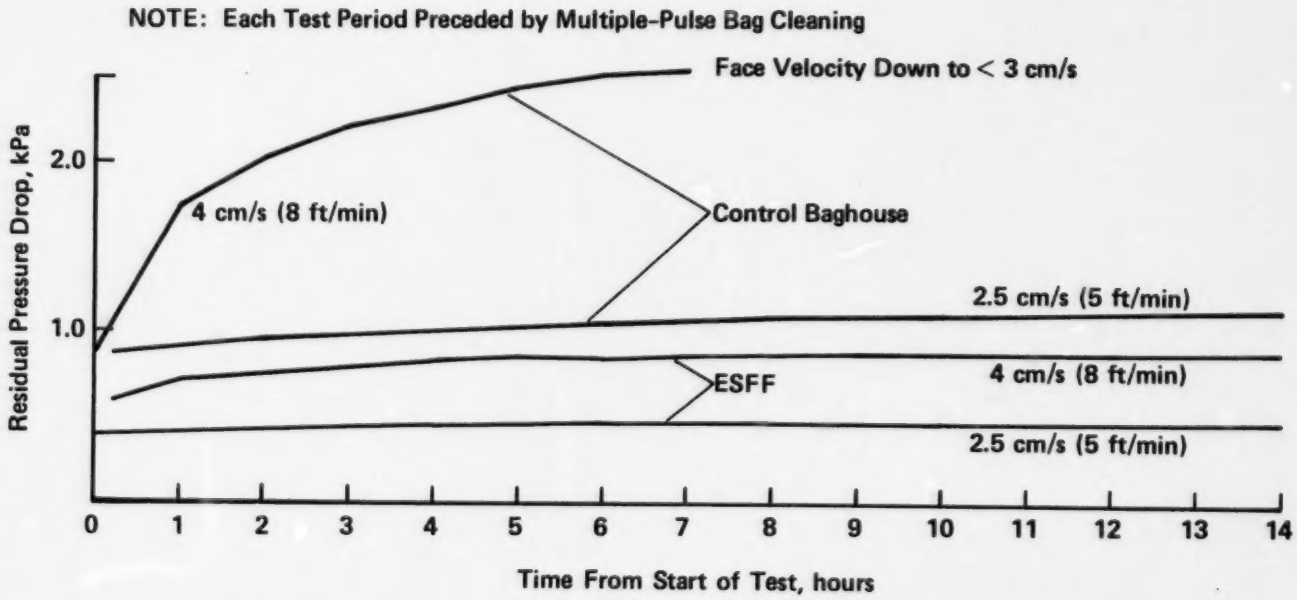

Figure 18. Residual pressure drop at two face velocities.

A test of increased face velocity operation was conducted during January of 1981; the results are presented in Figures 19a, 19b, and 19c. The control baghouse was operated at 2 cm/s (4 ft/min), a face velocity at which this baghouse was known to be stable. The ESFF baghouse was operated at 2-, 3-, 4-, and 5-cm/s face velocities (4-, 6-, 8-, and 10-ft/min). The initial ESFF residual pressure drop is quite low because the ESFF bags were replaced January 12, 1981.

The new bags were conditioned at 2 and 4 cm/s and tested on a longer term basis beginning January 16, 1981. The initial test was run at 3 cm/s (6 ft/min) with a 30-min pulse cleaning cycle and a field strength of 3.6 kV/cm. As can be seen from Figure 19a, the ESFF baghouse achieved stable operation. At noon on January 19, 1981, the face velocity of the ESFF baghouse was raised to 4 cm/s (8 ft/min). The ESFF baghouse operated well while on a 15-min or less cleaning cycle. Operation with a 30-min cleaning cycle was not successful at 4 cm/s (8 ft/min). Total operating time at 4 cm/s (8 ft/min) was 7 days. Field strength was 3.6 kV/cm. The ESFF baghouse was operated at 5 cm/s for 2 days beginning January 26, 1981. The cleaning cycle was 10 min in duration and the ESFF field strength was again 3.6 kV/cm.

In summary, the electrically augmented baghouse appears to be capable of operation at face velocities above those normally used for pulse-jet baghouses.

PARTICULATE REMOVAL EFFICIENCY

Particulate collection efficiency was studied using both EPA Method 5 tests and cascade impactor tests. Table 9 is a presentation of the Method 5 test results for the pilot baghouses. The average efficiency for the ESFF baghouse was 98.0 percent with an average outlet of 0.017 g/sm^3 (0.0076 gr/scf). The control baghouse averaged an outlet loading of 0.016 g/sm^3 (0.0069 gr/scf) and an efficiency of 98.9 percent. These values are essentially identical; the pilot unit data do not show a conclusive particulate mass removal advantage (based on Method 5 data) for either baghouse. Figure 20 is a plot of control inlet mass loadings versus ESFF inlet mass loadings for tests run simultaneously. Overall, the average ESFF inlet mass

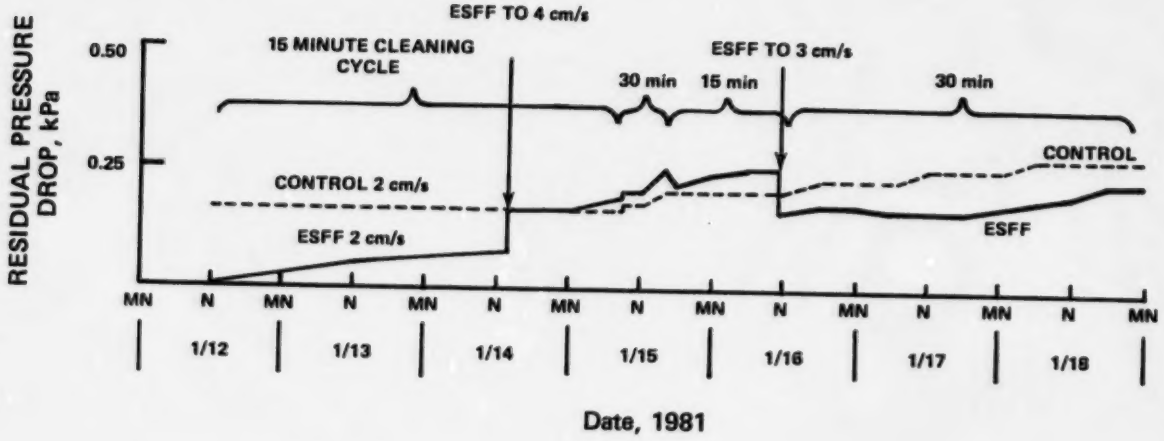

Figure 19a. Residual pressure drop for January 12-18, 1981.

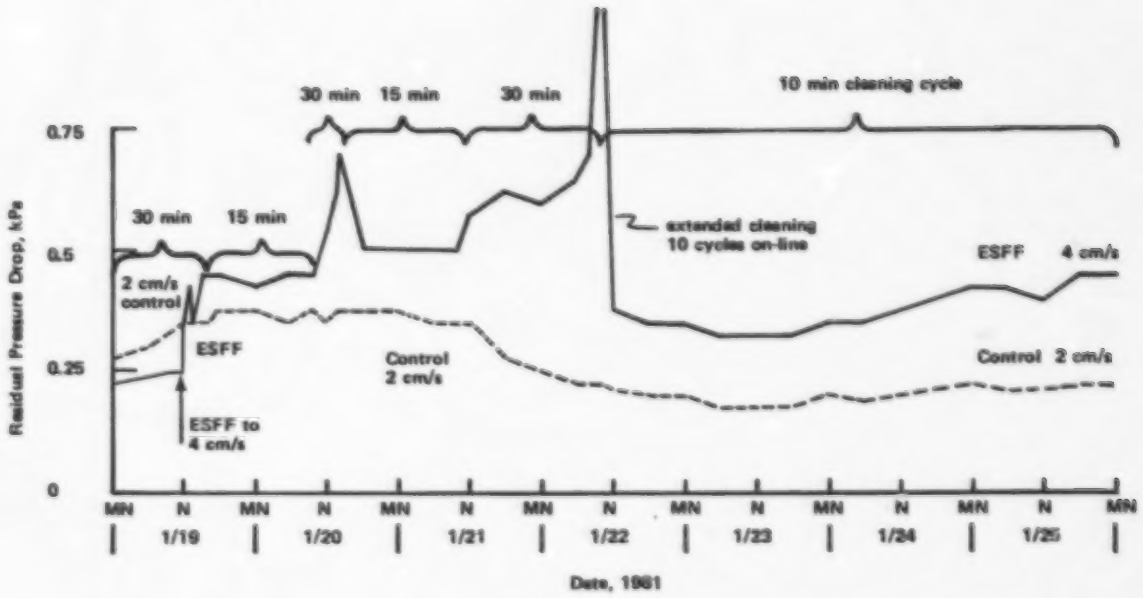

Figure 19b. Residual pressure drop for January 19-25, 1981.

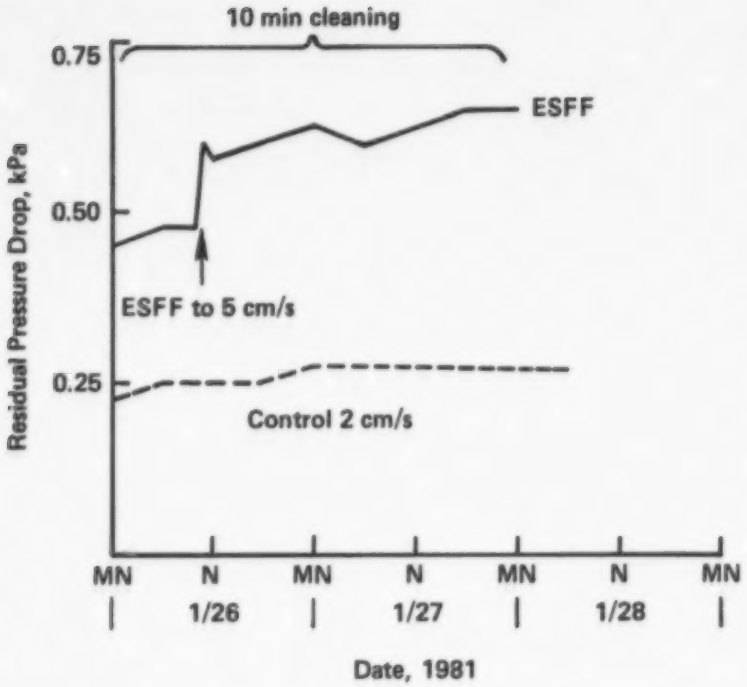

Figure 19c. Residual pressure drop for January 26-28, 1981.

TABLE 9. METHOD 5 TESTS RESULTS

Date	Run No.	Description	Face velocity		Mass concentration		Efficiency (simultaneous tests)
			cm/s	ft/min	g/sm³	gr/scf	
6/17/80	4A	INLET ESFF	3.2	6.3	1.67	0.73	
6/17/80	4B	INLET CONTROL	3.0	6.0	1.44	0.63	
7/01/80	5A	INLET ESFF	2.0	4.0	0.64	0.28	
7/01/80	5B	INLET CONTROL	2.0	4.0	0.54	0.24	
7/09/80	6A	OUTLET ESFF	3.0	6.0	0.0025	0.0011	
7/09/80	6B	OUTLET CONTROL	3.0	6.0	0.0048	0.0021	
7/30/80	7A	INLET ESFF	3.0	6.0	0.69	0.302	>0.984
7/30/80	7B	OUTLET ESFF	3.0	6.0	0.011	0.005	
7/31/80	8A	INLET CONTROL	3.0	6.0	2.46*	1.008*	>0.996*
7/31/80	8B	OUTLET CONTROL	3.0	6.0	0.009	0.004	
1/08/81	9A	INLET ESFF	3.0	6.0	1.008	0.441	>0.982
1/08/81	9B	OUTLET ESFF	3.0	6.0	0.018	0.008	
1/08/81	10A	INLET ESFF	3.0	6.0	0.93	0.406	>0.983
1/08/81	10B	OUTLET ESFF	3.0	6.0	0.016	0.0068	
1/09/81	11A	INLET CONTROL	2.0	4.0	1.206	0.527	>0.992
1/09/81	11B	OUTLET CONTROL	2.0	4.0	0.009	0.004	
1/20/81	12A	INLET ESFF	4.0	8.0	0.87	0.38	>0.977
1/20/81	12B	OUTLET ESFF	4.0	8.0	0.02	0.009	
1/20/81	13A	INLET ESFF	4.0	8.0	0.67	0.29	>0.955
1/20/81	13B	OUTLET ESFF	4.0	8.0	0.03	0.013	
1/21/81	14A	INLET CONTROL	2.3	4.6	0.68	0.30	>0.988
1/21/81	14B	OUTLET CONTROL	2.5	5.1	0.008	0.0035	
1/21/81	15A	INLET CONTROL	2.3	4.6	0.694	0.303	>0.988
1/21/81	15B	OUTLET CONTROL	2.5	5.1	0.008	0.0034	
1/29/81	16A	INLET ESFF	4.0	8.0	0.42	0.183	
1/29/81	17A	INLET CONTROL	2.0	4.0	0.42	0.182	
2/03/81	18B	OUTLET CONTROL	2.0	4.0	0.015	0.0064	
2/03/81	19B	OUTLET ESFF	2.0	4.0	0.14	0.062	ELEC ON/OFF
2/04/81	20B	OUTLET ESFF	2.0	4.0	0.11	0.048	NO CLEAN
2/04/81	21B	OUTLET CONTROL	2.0	4.0	0.015	0.0067	NO CLEAN
2/04/81	22B	OUTLET CONTROL	2.0	4.0	0.010	0.0046	10 MIN CLEAN
2/04/81	23B	OUTLET ESFF	2.0	4.0	0.21	0.0934	ELEC OFF
2/05/81	24B	OUTLET CONTROL	2.0	4.0	0.062	0.027	
2/06/81	25B	OUTLET ESFF	2.0	4.0	0.024	0.0107	ELEC ON

* Possible experimental error.

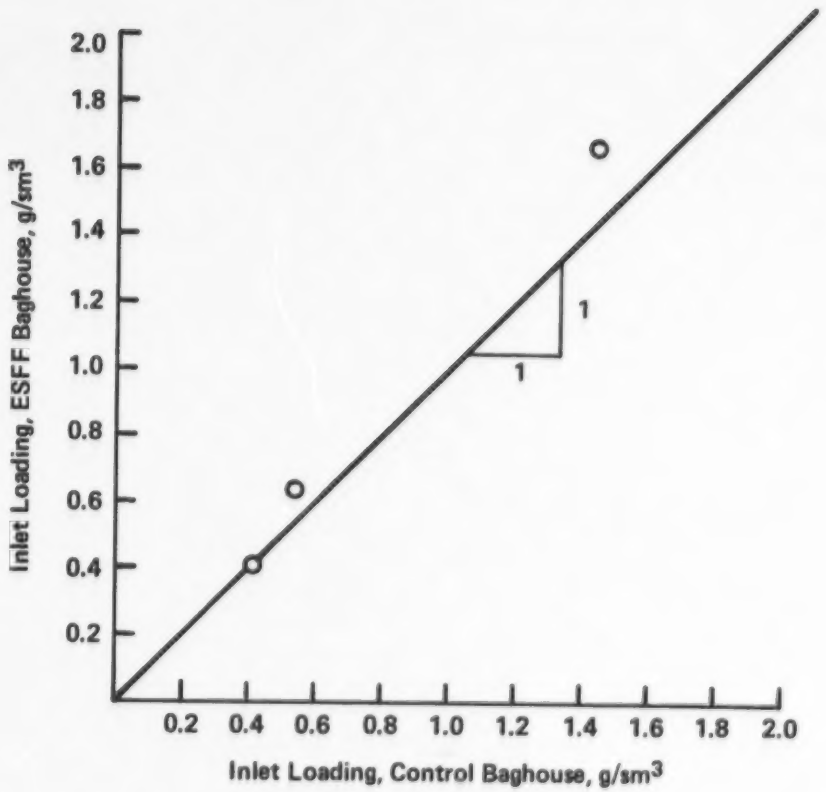

Figure 20. Inlet mass concentration comparison for ESFF and control baghouses.

loading was 0.86 g/sm^3 with an estimated standard deviation of 0.38, while the control inlet averaged 0.83 g/sm^3 with a standard deviation of 0.40 (not including run 7A).

The average cumulative particle size distributions for the two baghouses are presented in Figure 21. The data were taken over 3 days with the indicated number of runs. The ESFF and control inlet distributions and the ESFF inlet and outlet distributions did not differ significantly when tested at the 90-percent confidence level. The control outlet distribution differed significantly from the control inlet at particle diameters greater than 1 μm and from the ESFF outlet at particle diameters greater than 4 μm (again, at the 90-percent confidence interval). Figure 22 is the average penetration plot for both baghouses. The advantage shown for the ESFF baghouse is contrast to the lack of advantage indicated by the Method 5 test work. During the test period, the control baghouse was cleaning much more frequently than was the ESFF baghouse, which may have led to increased penetration due to seepage.

FABRIC EFFECTS

Fabric-dependent results of the pilot plant test work were presented earlier in Figure 15. The two Teflon® fabrics behave identically with respect to PDR and are not identified separately in other data presentations for that reason. In addition, PDR results achieved with the standard Teflon® (not napped) break-in bags were essentially identical to these results. In summary, identical PDR results were achieved with standard 23-oz Teflon® felt, 23-oz Teflon® felt which was mechanically napped, and a 17-oz Teflon® felt which was needled to only one side of the scrim. Particulate removal data are inadequate to detect differences between fabrics.

The fiberglass fabric PDR results are considerably less impressive than the Teflon® fabric PDRs. This result is consistent with laboratory work by TRI, but the difference between Teflon® and fiberglass was much greater in the pilot unit than was true in the laboratory. As the test period for fiberglass was only about 3 weeks, the data base is small. Fiberglass fabrics are not generally used in pulse-cleaned baghouses, but the data give some indication of what might be expected from a fiberglass-bag reverse-air unit.

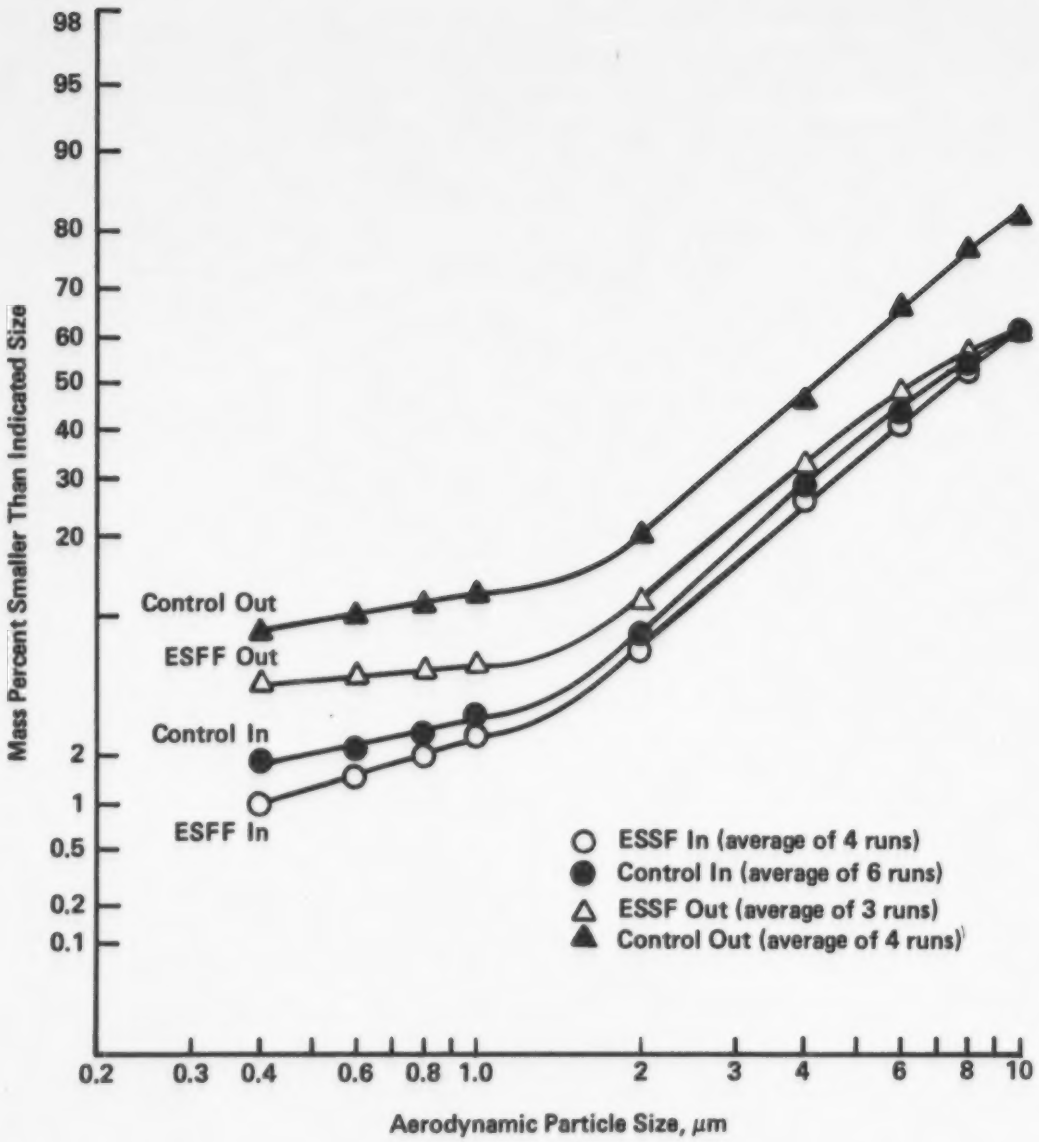

Figure 21. Inlet and outlet cumulative size distributions.

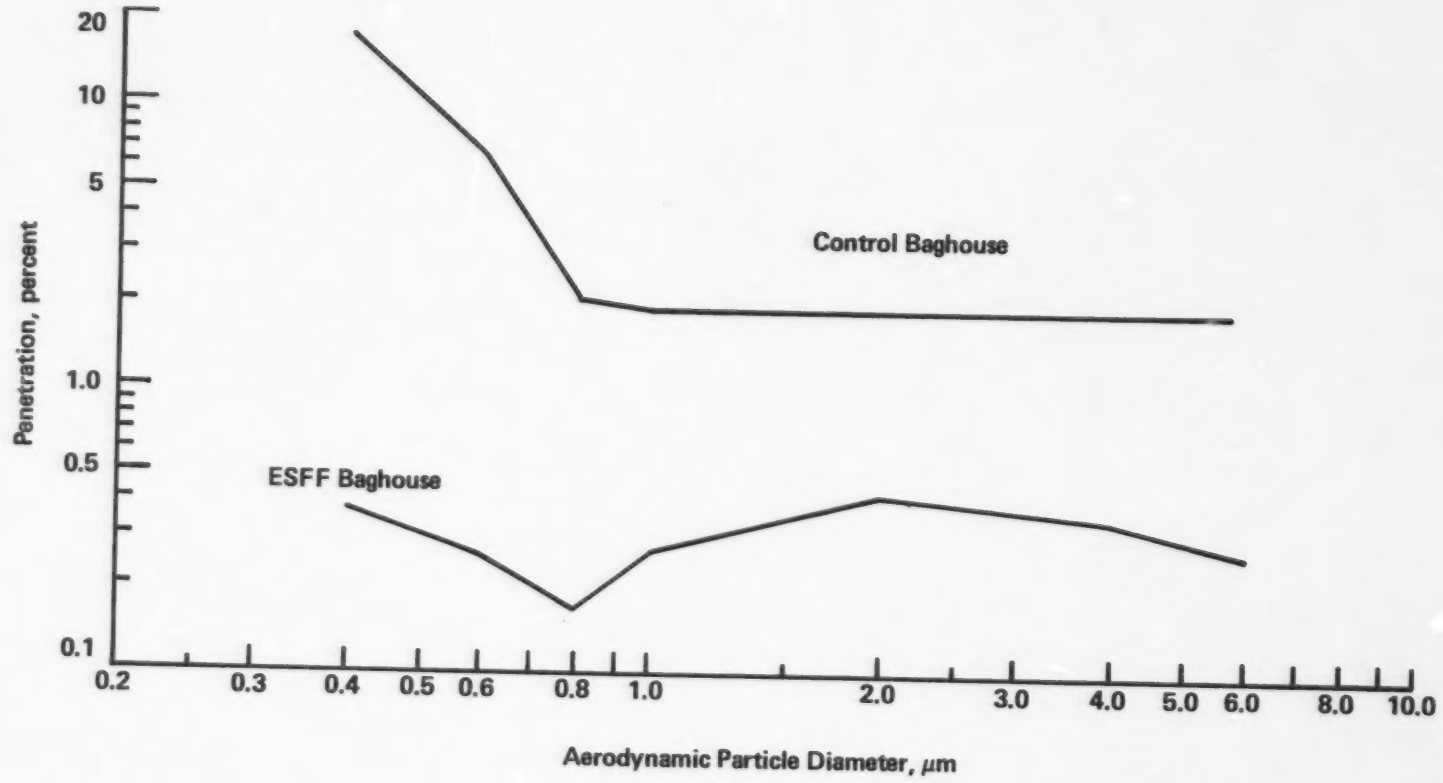

Figure 22. Average size-dependent particle penetration.

ELECTRICAL REQUIREMENTS

The total current range under normal operating conditions was nearly zero to about 200 μA. The outside harness electrodes, embedded in the dust cake on the outside of the bag, averaged about 50 μA and ranged up to 100 μA at times with stable operation. Current was roughly proportional to voltage for the outside electrodes. The inside cage/electrode combination averaged only 10 to 20 μA when operating, ranging down to nearly zero μA on some days, and the current was not affected greatly by voltage over the operating range. The currents were fairly stable within a day, although some drift did occur.

Power requirements at the field strengths and currents above amount to about 0.5 to 1.0 W/m^2 (0.05 to 0.1 W/ft^2).

SECTION 8

ECONOMICS

INTRODUCTION

The results presented in the preceding section suggest that the application of ESFF to pulse-jet baghouses might be economically advantageous. A preliminary economic study was conducted to further evaluate the ESFF concept and to identify the economically optimal modes of operation.

Cost estimates were made for both pulse-jet and reverse-air baghouses. The pulse-jet baghouse operating conditions are based on pilot unit results. The reverse air operating conditions estimated are not at this time supported by experimental data but are estimated from the pulse-jet results.

ANALYTICAL METHODS

The economic potential of the ESFF concept was explored by comparing the total annual costs of a conventional baghouse filter with a similar filter equipped with ESFF hardware. The study assumes that the dust being controlled is fly ash from a pulverized coal boiler.

Total annual costs consisted of the annual capital costs plus the annual operating costs. Assumptions made in developing the cost elements are discussed separately in the following paragraphs.

Annual Capital Costs

An annual capital cost was developed to include all flange-to-flange hardware for the baghouse except the bags. Since the bag cost and bag life were variables in this study, they were treated separately as operating costs.

$$\text{Annual Capital Cost (C) is: } C = (CFR + TI)\ 3.28\ Q, \frac{\$}{yr\text{-}m^2} \qquad (9)$$

$$\text{where CFR (Capital Recovery Factor)} = \frac{i\ (1 + i)^N}{(1 + i)^N - 1}$$

i = interest rate, fraction

N = depreciation life, years

TI = taxes and insurance, fraction if installed cost

Q = manufacturer's selling price, dollars/m^2 collector

3.28 = installed cost factor (see Table 10).

For this study, the following values were used:

i = 0.14

N = 15 years

TI = (0.04) (installed cost)

thus: $C = 0.666\ Q$, \$/yr-m^2.

A manufacturer's selling price was arrived at by the estimate shown in Table 11. This estimate is compared with estimates from two vendors, as shown at the bottom of Table 11. For the pulse-cleaned conventional baghouse, a manufacturer's selling price (Q) of \$161.50/m^2 was used; a cost of \$183.00/m^2 was used for the ESFF baghouse.

The reverse-air baghouse costs were not estimated at the same level of detail as were the pulse-jet costs. A new 100-MW power plant was estimated to have a flue gas flow of 8740 m^3/min using the values from midwestern coal.[23] Based on a similarly sized reverse-air-cleaned baghouse installed in the spring of 1980, an installed capital cost of \$258.00/m^2 of cloth (equipment cost of \$78.70/m^2) was used. The ESFF baghouse cost was assumed to be in the same ratio for the reverse-air baghouse as was estimated for the pulse-jet baghouse. The purchased equipment cost for ESFF was then estimated to be:

$$Q = \frac{\$183.00}{\$161.50} \quad \$78.70/m^2$$

$$Q_{ESFF} = \$89.20/m^2 \qquad (10)$$

TABLE 10. INSTALLED COST FACTORS AS A FUNCTION OF EQUIPMENT COST Q[22]

Component	Direct costs	
	Material	Labor
Equipment	1.00Q	0.25Q
Ductwork	0.04Q	0.21Q
Instrumentation	0.04Q	0.006Q
Electrical	0.11Q	0.16Q
Foundations	0.03Q	0.05Q
Structural	0.03Q	0.05Q
Sitework	0.02Q	0.02Q
Painting	0.004Q	0.02Q
Total direct costs	1.27Q	0.77Q

Component	Indirect costs	
	Measure of costs	Factor
Engineering	10% material and labor	0.204Q
Contractor's fee	10% material and labor	0.306Q
Shakedown	5% material and labor	0.102Q
Spares	1% material	0.013Q
Freight	3% material	0.038Q
Taxes	3% material	0.038Q
Total indirect costs		0.70Q
Contingencies - 20% of direct and indirect costs		0.54Q
Total capital costs		3.28Q

TABLE 11. COST ESTIMATE FOR A PULSE-CLEANED BAGHOUSE HAVING 225 15.24-cm (6-in.) DIAMETER BY 4.3-m (14-ft) BAGS (460 m^2 OF CLOTH)

	Conventional	ESFF
Metal	$20,000	$20,000
Insulation	8,000	8,000
Structural	4,000	4,000
Ash valves	1,000	1,000
Cages	3,400	10,000
Platforms	1,000	1,000
Inlet and outlet ducts	2,500	2,500
In and out valves	2,000	2,000
Pulse valves	1,500	1,500
Electrical and instrumentation	-0-	2,000
	$43,400	$52,000
Manufacturing profit & OH @ 40%	$17,360	$20,800
Contingency @ 20%	8,680	10,400
	$69,440	$83,200
Unit manufacturer's selling price:	$151.00/$m^2$	$180.90/$m^2$
Vendor No. 1 estimate = $\frac{\$60,000}{371.6\ m^2}$:	$161.50/$m^2$	
Vendor No. 2 estimate = $\frac{\$79,750}{418.1\ m^2}$:	$190.80/$m^2$	
Base estimates on:	$161.50/$m^2$	$183.00/$m^2$

Annual Operating Cost

Annual operating cost was assumed to include four components: (1) fan electrical power cost, (2) cleaning system electrical power cost, (3) equipment maintenance, and (4) bag replacement. No increased electrical cost was assigned to the ESFF baghouse, as pilot-plant experience has shown it to be negligible. The capacity factor was assumed to be one and fan efficiency to be 82 percent.

$$\text{Fan Power} = 194.94\ (\$/kWh)(\Delta P)(G/C),\ \$/m^2\text{-yr}$$

$$G/C = \text{face velocity, cm/s}$$

$$\$/kWh = \text{electrical power cost}$$

$$\Delta P = 0.75 + C_1(G/C),\ kPa$$

where C_1 = average fabric presssure drop factor, kPa/(cm/s).

This pressure drop equation predicts the overall drop through the complete control device. The "0.75 kPa" drop is for ductwork. The "$C_1(G/C)$" term accounts for the average drop that exists across the baghouse and includes both the clean bag resistance and the dust cake resistance at its average value.

$$\text{Cleaning Power} = 0.10 \times \text{fan power},\ \$/m^2\text{-yr}$$

$$\text{Annual Maintenance} = 0.03 \times \text{manufacturer's selling price}$$

$$= 0.03Q,\ \$/m^2\text{-yr}$$

$$\text{Annual Bag Replacement Cost} = \left(\frac{i\ (1 + i)^L}{(1 + i)^L - 1}\right) B,\ \$/m^2\text{-yr}$$

$$= FB,\ \$/m^2\text{-yr}$$

where i = interest rate, fraction

L = bag life, years

B = bag cost, $\$/m^2$

F = bag replacement factor.

Calculation Method

Combining capital and operating costs results in the following equation:

$$TAC = \frac{1.16\ Q}{G/C} + \frac{1.667\ FB}{G/C} + 194.94\ (\$/kWh)[0.75 + C_1\ (G/C)] \quad (11)$$

where TAC = total annual cost, $\$/(m^3/min)$-yr.

This equation was repetitively solved, using a programmable calculator, for a range of variables. Tables 12, 13, and 14 present solutions to the cost equations for various values of the parameters.

RESULTS

Pulse-Jet Baghouse

All of the pilot-unit experience to date has been with a pulse-jet baghouse. The bags have been Teflon® felt for the majority of the test program. A bag cost of \$48.44 m^2 (\$4.50/ft^2) and a life of 4 years was chosen as reasonable for this type of operation. A conventional pulse-jet might well be designed to operate at an overall ΔP of 2.25 kPa (9 in. H_2O) with a 2-cm/s (4-ft/min) face velocity, although that would be the high end of its proven capabilities. The "conventional" line on Figure 23 is for this pulse-jet baghouse. Extended operation at the pilot unit, as presented in Section 7 (Operation at Increased Face Velocity), gave considerable evidence that the ESFF baghouse can be expected to operate within the ΔP formula used for the data in Figure 23 up to a face velocity of about 4 cm/s (8 ft/min).

Figure 23 shows clearly the potential savings associated with the ESFF concept. At a face velocity of 2 cm/s (4 ft/min) and \$0.03/kWh, the ESFF baghouse has a higher total annual cost because of its higher capital cost. The ESFF annual cost becomes less than the conventional baghouse at 2 cm/s as electrical costs increase. At face velocities of 3 and 4 cm/s, the ESFF baghouse has a clear advantage. Even if operation at 4 cm/s over the life of a baghouse is considered too optimistic, operation at 3 cm/s will save nearly \$40,000 annually for \$0.05/kWh electricity. Similar curves can be drawn for other values of the parameters.

TABLE 12. CONVENTIONAL PULSE-JET BAGHOUSE--EQUIPMENT COST $161.50/m^2$

Face velocity, G/C (cm/s)	Total annual cost, $/(m³/min)-yr											
	Teflon® bags @ $48.44/m²						Glass bags @ $4.84/m²					
	2-yr bag life			4-yr bag life			2-yr bag life			4-yr bag life		
	Elec. cost, $/kWh			Elec. cost, $/kWh			Elec. cost, $/kWh			Elec. cost, $/kWh		
	0.03	0.05	0.10	0.03	0.05	0.10	0.03	0.05	0.10	0.03	0.05	0.10
1	245.00	251.00	265.00	224.00	229.00	244.00	201.00	207.00	221.00	199.00	204.00	219.00
2	131.00	140.00	162.00	121.00	129.00	151.00	109.00	118.00	140.00	108.00	117.00	139.00
3	96.30	108.00	137.00	89.10	101.00	130.00	81.60	93.20	122.00	80.80	92.50	122.00
4	81.00	95.60	132.00	75.60	90.20	127.00	69.90	84.60	121.00	69.40	84.00	120.00
5	73.60	91.10	135.00	69.30	86.80	130.70	64.70	82.30	126.00	64.30	81.80	126.00

$\Delta P = 0.75 + 0.75\ (G/C)$, kPa

TABLE 13. ESFF PULSE-JET BAGHOUSE--EQUIPMENT COST $183/m^2$

Face velocity, G/C (cm/s)	Total annual cost, $/(m³/min)-yr											
	Teflon® bags @ $48.44/m²						Glass bags @ $4.84/m²					
	2-yr bag life			4-yr bag life			2-yr bag life			4-yr bag life		
	Elec. cost, $/kWh			Elec. cost, $/kWh			Elec. cost, $/Kwh			Elec. cost, $/kWh		
	0.03	0.05	0.10	0.03	0.05	0.10	0.03	0.05	0.10	0.03	0.05	0.10
1	267.00	271.00	280.00	246.00	250.00	259.00	223.00	227.00	236.00	221.00	224.00	234.00
2	138.00	148.00	155.00	127.00	132.00	144.00	116.00	121.00	133.00	115.00	120.00	132.00
3	95.80	102.00	116.00	88.70	94.50	109.00	81.10	86.90	102.00	80.40	86.20	101.00
4	76.50	82.30	99.40	70.70	77.00	94.00	64.50	71.30	88.30	63.90	70.80	87.80
5	63.90	71.71	91.20	59.60	67.40	86.90	55.10	62.90	82.40	54.70	62.50	82.00

$\Delta P = 0.75 + 0.25\ (G/C)$, kPa

TABLE 14. REVERSE-AIR BAGHOUSE--TOTAL ANNUAL COST, $/(M³/MIN)-YR

Face velocity, G/C (cm/s)	Control house, Q = $78.70/m²						ESFF house, Q = $89.20/m²					
	2-yr bag life			4-yr bag life			2-yr bag life			4-yr bag life		
	Elec. cost, $/kWh			Elec. cost, $/kWh			Elec. cost, $/kWh			Elec. cost, $/kWh		
	0.03	0.05	0.10	0.03	0.05	0.10	0.03	0.05	0.10	0.03	0.05	0.10
1	105.00	111.00	125.00	103.00	108.00	123.00	116.00	120.00	133.00	113.00	118.00	130.00
1.25	86.70	93.30	110.00	85.00	91.60	108.00	94.60	100.00	113.00	92.90	98.30	112.00
1.5	75.00	82.30	101.00	73.60	80.90	99.20	80.90	86.80	101.00	79.50	85.40	100.00
2	61.20	70.00	91.90	60.10	68.90	90.80	64.40	71.20	88.20	63.30	70.10	87.20

Assuming glass bags @ $4.84/m².

$\Delta P_{conventional} = 0.75 + 0.75\ (G/C)$, kPa

$\Delta P_{ESFF} = 0.75 + 0.5\ (G/C)$, kPa

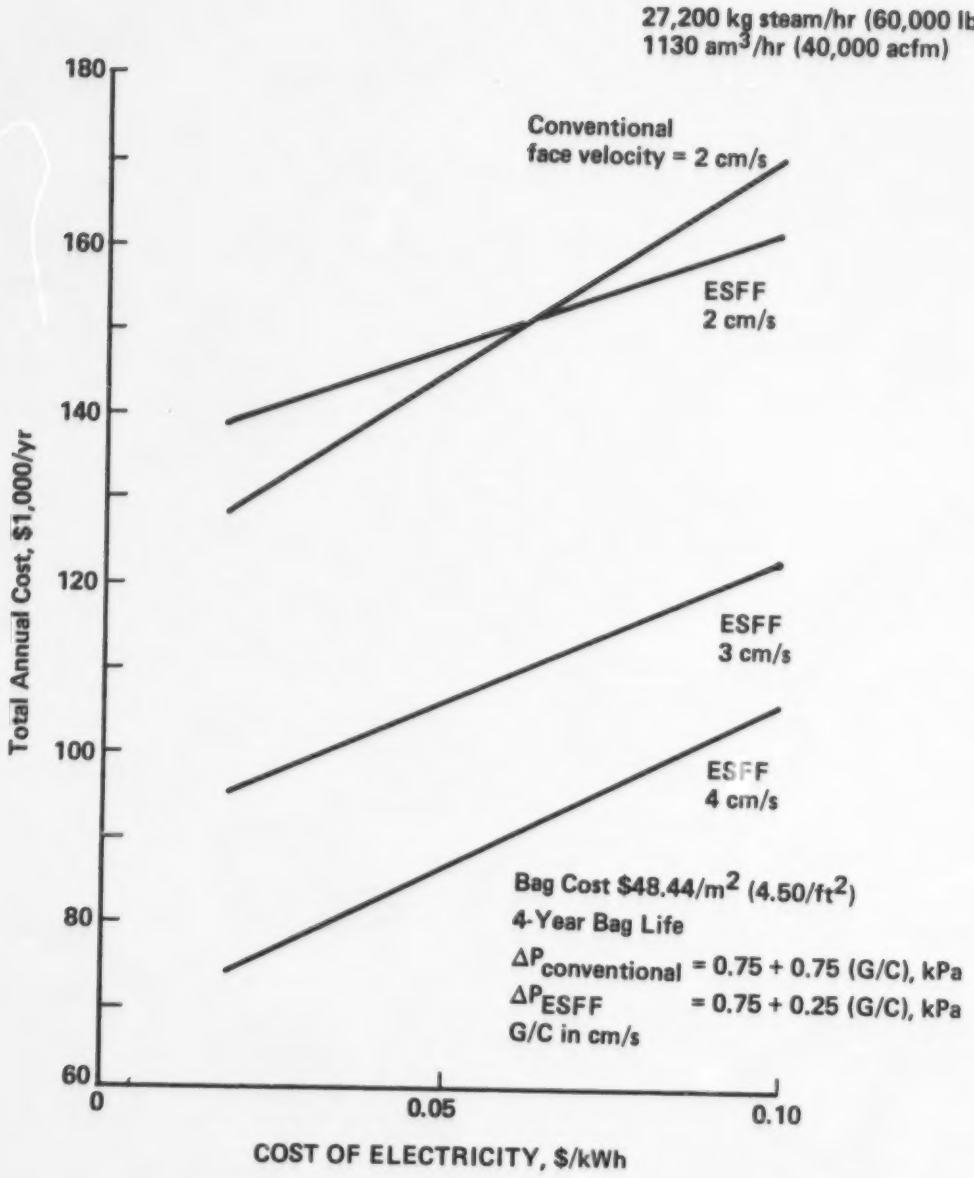

Figure 23. Pulse-jet baghouse cost: pulverized coal industrial boiler.

Reverse-Air Baghouse

No operating experience is yet available with an ESFF reverse-air cleaned house. The data that are available with glass bags indicate that the effect is not so great as with the napped Teflon® bags. The costs shown in Figure 24 should be considered to be less reliable than those for the pulse jet. The plot is still meaningful, however, as it shows again the potential advantages of ESFF. If reverse-air ESFF shows the same resistance to fabric blinding that has been evident with the pulse-jet unit, operation at the increased gas/cloth ratios will be possible, and considerable savings will result.

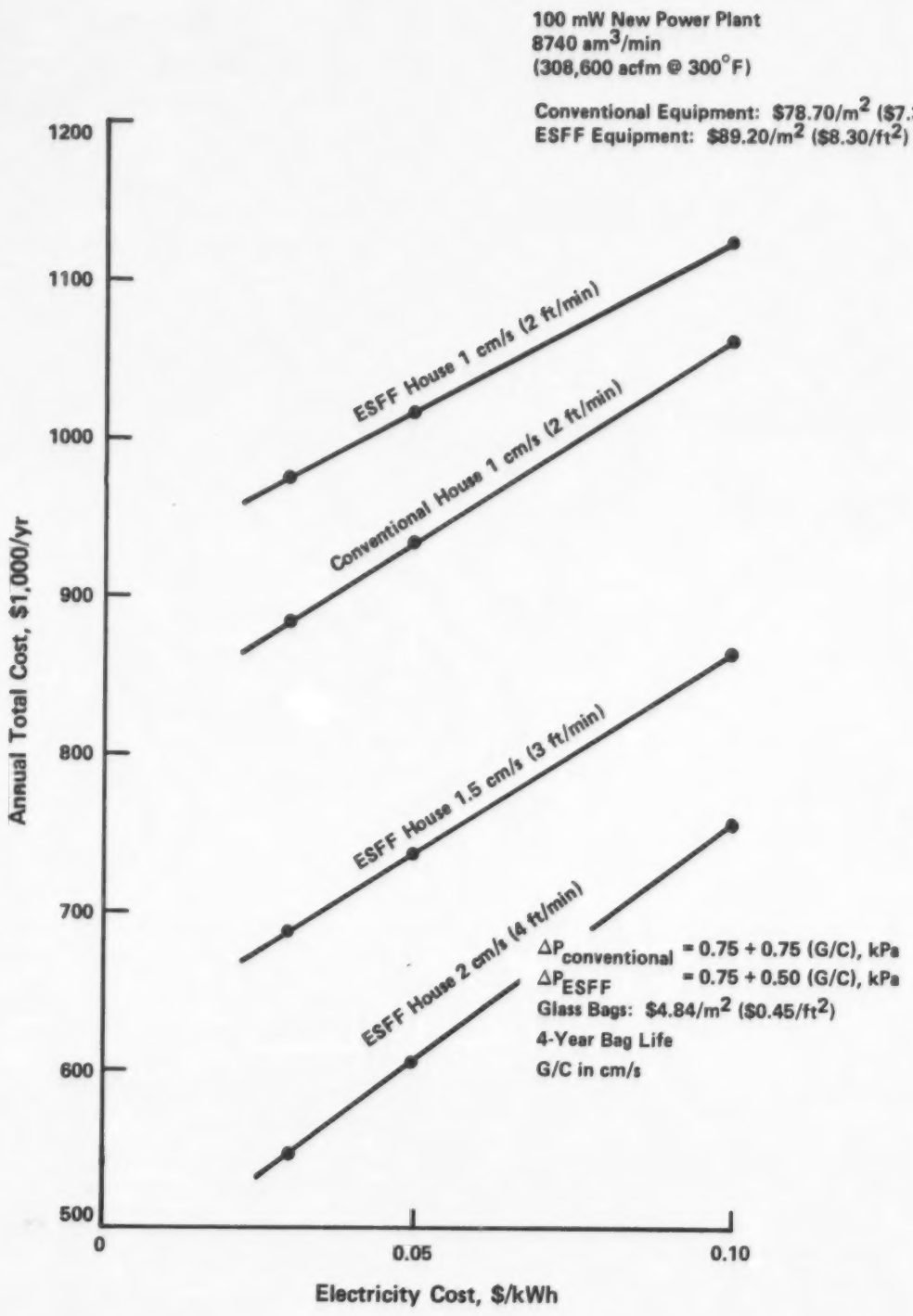

Figure 24. Reverse-air baghouse cost: power plant.

SECTION 9

REFERENCES

1. Cooper, D. W. Mechanisms for Electrostatic Enhancement of Filter Performance. Invited paper presented to The Fiber Society and the Filtration Society Joint Symposium on Fibers, Electrostatics and Filtration, Princeton, New Jersey, November 14-15, 1979.

2. Wang, C. S., and C. P. Ho. Inertial and Electrostatic Deposition of Solid Particles on Isolated Fibers. Invited paper presented to The Fiber Society and the Filtration Society Joint Symposium on Fibers, Electrostatics and Filtration, Princeton, New Jersey, November 14-15, 1979.

3. Wang, C. S., C. P. Ho, H. Makino, and K. Iinoya. Effect of Electrostatic Fields on Accumulation of Solid Particles on Single Cylinders. AIChE Journal, 26(4):680-685, July 1980.

4. Oak, M. J., and D. A. Saville. Dendrite Structures in Electrically Stimulated Filtration. Invited paper presented to The Fiber Society and the Filtration Society Joint Symposium on Fibers, Electrostatics and Filtration, Princeton, New Jersey, November 14-15, 1979.

5. Donovan, R. P., J. H. Turner, and J. H. Abbott. Passive Electrostatic Effects in Fabric Filtration. In: Second Symposium on the Transfer and Utilization of Particulate Control Technology, Volume I. EPA-600/9-80-039a (NTIS PB 81-122202), U. S. Environmental Protection Agency, September 1980. pp. 476-493.

6. Helfritch, D. J. Apitron Product Brochure, 1979. Apitron Division, American Precision Industries, 12037 Goodrich Drive, Charlotte, North Carolina 28217.

7. Ariman, T., and D. J. Helfritch. Pressure Drop in Electrostatic Fabric Filtration. In: Second Symposium on the Transfer and Utilization of Particulate Control Technology, Volume III. EPA-600/9-80-039c, U. S. Environmental Protection Agency, September 1980. pp. 222-236.

8. Iinoya, K., and Y. Mori. Effects of a Corona Precharger and Relative Humidity on Filter Performance. In: Second Symposium on the Transfer and Utilization of Particulate Control Technology, Volume III. EPA-600/9-80-039c, U. S. Environmental Protection Agency, September 1980. pp. 237-250.

9. Chudleigh, P. W., and N. W. Bainbridge. Electrostatic Effects in Fabric Filters During Build-Up of the Dust Cake. Filtration and Separation, 17:309-311, July/August 1980.

10. Nelson, G. O., et al. Enhancement of Air Filtration Using Electric Fields. Am. Ind. Hyg. Assoc. J., 39:472-479, June 1978.

11. Walkenhorst, W., and G. Zebel. Uber ein neues Schwebstoffilter hoher Abscheideleistung and geringen Strömungswiderstandes. Staub-Reinhalt, Luft 24:444-448, 1964.

12. Zebel, G. Deposition of Aerosol Flowing Past a Cylindrical Fiber in a Uniform Electric Field. J. Colloid Science, 20:522-543, 1965.

13. Rivers, R. D. Operating Principles of Non-Ionizing Electrostatic Air Filters. ASHRAE, 4:37-40, February 1962.

14. Penney, G. W. Using Electrostatic Forces to Reduce Pressure Drop in Fabric Filters. Powder Technology, 18:111-116, 1977.

15. Penney, G. W. Electrostatic Effects in Fabric Filtration: Volume I. Fields, Fabrics and Particles (Annotated Data). EPA-600/7-78-142a (NTIS PB 288576), U. S. Environmental Protection Agency, September 1978.

16. Lamb, G. E. R., and P. A. Costanza. Electrical Stimulation of Fabric Filtration. Textile Research Journal, 47:372-380, May 1977.

17. Lamb, G. E. R., and P. A. Costanza. Electrical Stimulation of Fabric Filtration: Part II. Textile Research Journal, 48:566-573, October 1978.

18. Lamb, G. E. R., and P. A. Costanza. A Low-Energy Electrified Filter System. Filtration and Separation, 17:319-322, July/August 1980.

19. Marcotte, W. R. Fabric Filter Experience at Waynesboro. In: Second Symposium on the Transfer and Utilization of Particulate Control Technology, Volume I. EPA-600/9-80-039a (NTIS PB 81-122202), U. S. Environmental Agency, September 1980. pp. 372-389.

20. Bickelhaupt, R. E. A Technique for Predicting Fly Ash Resistivity. EPA-600/7-79-204, U. S. Environmental Protection Agency, August 1979.

21. Ensor, D. S., et al. Evaluation of the United McGill Electrostatic Precipitator. Report in preparation for the U. S. Environmental Protection Agency, to be published July 1981.

22. Cost Analysis Manual for Standards Support Document. Economics Analysis Branch, U. S. Environmental Protection Agency, Research Triangle Park, North Carolina.

23. McGlamery, G. C., et al. Economics and Energy Requirements of Sulfur Oxides Control Processes. Tennessee Valley Authority, Muscle Shoals, Alabama.

APPENDIX A

IMPACTOR TEST PROCEDURES

1. Obtain a duct center-line velocity and stack pressure. Use pitot tube for velocity and static probe for static pressure. Note duct orifice reading and maintain flow by orifice.

2. Compute the isokinetic sampling velocity for the duct of interest.

   a. The inlet with particulate concentrations of about 2 g/m^3 will require a smaller nozzle (~ 0.4 cm) and low sampling rates [roughly 0.01 m^3/min (0.4 scfm)]. A 0.170-in. nozzle prepared from a 0.25-in. tube is suitable. Also, short sampling times of a few minutes will be required. In some cases part of the last stage holes should be blocked to obtain the desired cutoff.

   b. The outlet of the control device will normally require a larger nozzle and higher flow rates to obtain acceptable quantities of material on the stages. Typically, flow rates of 0.05 to 1.2 m^3/s (0.5 to 0.7 acfm) should be used. The ETS Method 5 nozzles (0.232 in.) are suitable for the outlet.

3. The impactor train should be assembled as shown in Figure A-1. Use Teflon® tape to assemble the impactor and all fittings.

4. Fill in the data sheet. Note that for short runs, less than 10 minutes or so, it is useful to precalculate the dry gas meter readings expected every minute of the test to allow close control of the sampling run.

5. The whole impactor train must be leak tested before and after the test. This is accomplished by plugging the inlet with Teflon® tape or duct tape and turning on the train and carefully adjusting the valves to greater than 10 in. Hg vacuum. An acceptable leak rate is less than 0.02 acfm. The pretest leak check should be done both before and after preheating.

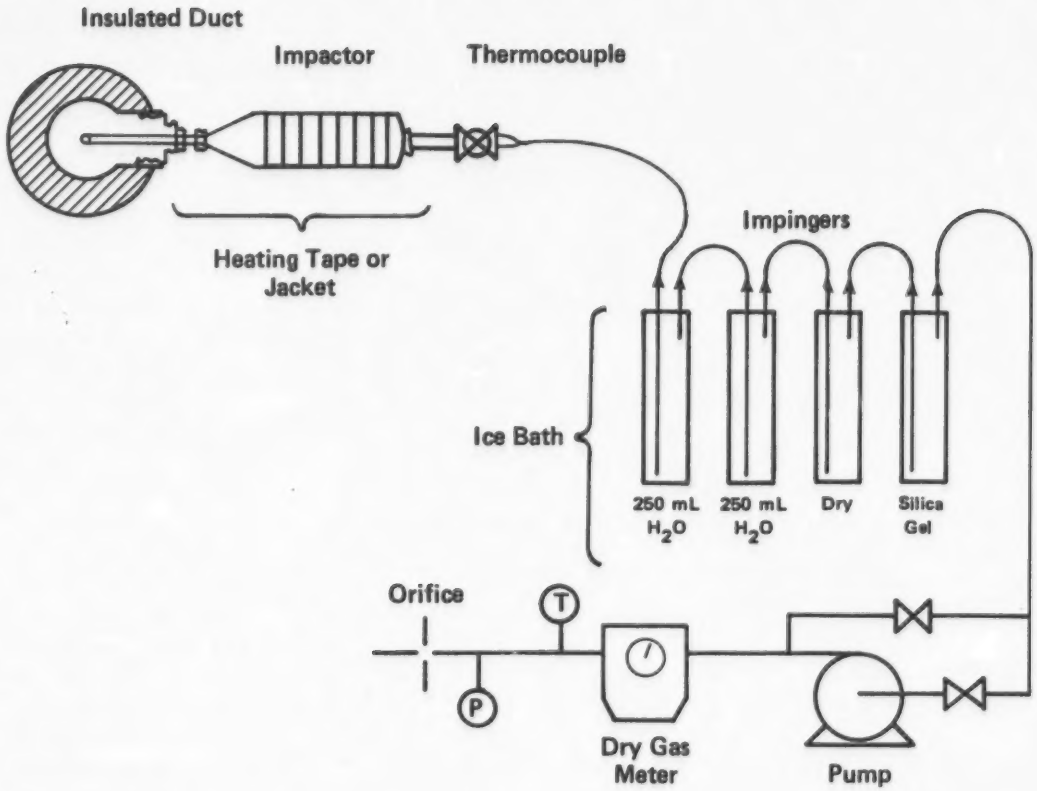

Figure A-1. Impactor train.

After the leak check, the flow valve should be preset to minimize problems during the test. For inlet runs, the flow must be preset. Care should be taken to avoid sucking impinger solutions back through the train. Release the vacuum from the nozzle first, then shut off the pump.

6. The impactor should be preheated until the thermocouple on the impactor is up to stack temperature and held at that temperature for 10 minutes. The valve on the impactor probe should be closed while preheating.

7. The run is started by inserting the nozzle into the duct, adjusting position to the center line, then opening the probe valve, and setting the desired flow rate. Normally the impactors are operated at one point in the duct.

8. During the run, record the test train parameters in systematic time intervals. (For example, in a 1-hour run, recordings should be made every 10 minutes.)

9. End the test by shutting off the pump and probe valve. Carefully remove the impactor from the port. Perform a post-test leak check.

10. Remove the hose and drain into the impinger. After the probe has cooled somewhat, remove the impactor and transport to the disassembly area.

LABORATORY PROCEDURES FOR MRI IMPACTORS AND PE AUTOBALANCE

General Notes

1. The balance power should remain ON at all times. When not in use the balance stirrups should be empty and the weighing chamber door closed.
2. Be gentle with the balance stirrups. They are delicate!
3. To avoid grease and dirt contamination, handle the balance tare weights and calibration weights with the separate tweezers found in the tare weight box.
4. Handle the substrates carefully with other tweezers; avoid touching the greased surfaces.

Daily Setup of Balance

1. Set FILTER on HI
2. Set RANGE on 200.
3. Zero display using COARSE and FINE zero knobs.

Daily Calibration of Balance

1. Place the 100 mg calibration weight on left stirrup.
2. When display stabilizes, adjust FINE CALIBRATION knob on back of control unit until display reads +100.00.

Loading Impactors

1. Be sure jet plates and substrates are in correct order.
2. Be sure all O-rings are in place.
3. Check the operating instructions and attach the correct probes to the impactors.
4. Inspect probe tips and repair or replace if necessary.

Unloading Impactors

1. Brush any loose particulate onto the next substrate below where the particulate is found.
2. Be careful not to lose portions of the filter when removing it.
3. Rinse out each probe with a few millileters of acetone and drain the acetone onto the appropriate cup. Air dry before placing cup into dessicator.
4. After rinsing, run a brush through each probe to dislodge any remaining material.
5. Check the condition of the dessicant in the dessicator and replace if necessary before storing substrates.

Sample Weighing (after overnight dessication)

1. Record the date of the weighing in the weighing book.
2. Remove the substrates from the dessicator one at a time and replace the cover of the dessicator.
3. To weigh substrates and probe cups:
   (a) Place the 500 mg and 200 mg tare weights on the right stirrup.
   (b) Place the sample on the left stirrup and close the chamber door.
   (c) When display stabilizes, record the number and sign.
4. To weigh filters:
   (a) Place the 100 mg tare weight on the right stirrup.
   (b) Place the filter on the left stirrup and close the chamber door.
   (c) When display stabilizes, record the number and sign.
5. Record any comments of interest next to the weights in the book.

IMPACTOR SUBSTRATE PREPARATION

1. Prepare a grease-toluene mixture to be spread on the substrate. For temperatures of 149° C (300° F) or above, use Apiezon H; otherwise Apiezon L may be used. When using Apiezon H, a 5% (by weight) solution of grease in toluene solution is appropriate. For Apiezon L, use 10% to 20% (by weight) grease in toluene.

2. Be sure that the impactor substrates are clean and dry. Place 25 to 30 substrates on an oven rack using tweezers (do not use your fingers). With an eyedropper put 5 or 6 drops on a substrate and spread the drops with a small paint brush to make an even coating. Do the substrates one at a time because the toluene in the solution evaporates quickly.

3. Bake the substrates at the temperature at which the impactor will be operated for at least 4 hours.

4. Desiccate the substrates for 12 to 24 hours.

5. Weigh the substrates and assign them to labeled petri dishes. Record the weight and petri dish.

QUALITY CONTROL PLAN

Substrate Weighing

1. The balance will be set up as described in the procedure.
2. The amount of zero and span drift will be recorded.
3. The balance will be checked with the reference substrate and the weight recorded. If the weight does not repeat within 0.03 mg, something is wrong with the balance.

Filters

1. To prevent spurious filter weight determinations, the glass fiber filters are to be conditioned in the flue gas at stack temperature for 2 to 4 hours.
2. The filters are placed in an insulated thimble holder shell which has been fitted with a prefilter and the prefilter with a nozzle. Outlet stack gas is drawn through the thimble holder at 0.2 to 0.4 acfm.
3. After preconditioning, the filters are immediately placed in the desiccator.

Blanks

1. An impactor blank is to be run every 10 to 20 runs. At least one blank must be run as part of any test series.
2. The blank run is identical to the other impactor tests except that the flue gas is filtered to remove particulate before the gas reaches the impactor.

APPENDIX B

CHARGE-TO-MASS MEASUREMENT OPERATING PROCEDURE

1. Filter Preparation

   a. Desiccate filters overnight at room temperature.

   b. Weigh and record weight.

2. Sampling

   a. Determine stack velocity with pitot tube and use static probe to get stack pressure.

   b. Calculate isokinetic sampling rate and select proper nozzle.

   c. Set up equipment as shown in Figure B-1. Put filter in filter holder and assemble apparatus. Preheat probe and Faraday cage to duct temperature.

   d. Fill out data sheet.

   e. Set electrometer for charge measurement and at proper scale (usually 10^{-7} Coul x 1 is appropriate) and recorder at 120 mV, 2.5 cm/min. Determine full scale deflection by changing electrometer scale ($\approx 10^{-11}$ Coul) and adjusting the zero to full meter deflection. Recorder should be about 85 percent of full scale. Reset electrometer scale to 10^{-7} Coul and zero meter. All fly ashes to date have been negative.

   f. Simultaneously start sampling and activate electrometer. May have to change polarity.

   g. As filter begins to load up, maintain flow rate. After collecting sufficient sample (≈ 50 mg), shut valve at back of Faraday cage. Avoid backflow in the impinger train.

   h. Carefully recover filter. Brush loose dust into the cup or petri dish if it is associated with the measured charge.

3. Sample Weighing

   a. Desiccate the samples overnight. Reweigh. Weigh blank as well as the samples.

4. Data Analysis

a. Determine total charge collected from electrometer and check against strip chart. Note that full scale on the electrometer is 1.0 x scale factor, not 10 as meter indicates (e.g., a final charge reading of 1.72 on the meter for scale of 10^{-7} Coul x 1 is a charge of 0.172×10^{-7} Coul). The recorder trace provides both a record of the final charge accumulation and a measure of the time dependence of the collected charge.

b. The charge-to-mass determination is made by dividing the total charge accumulated by the mass collected on the filter.

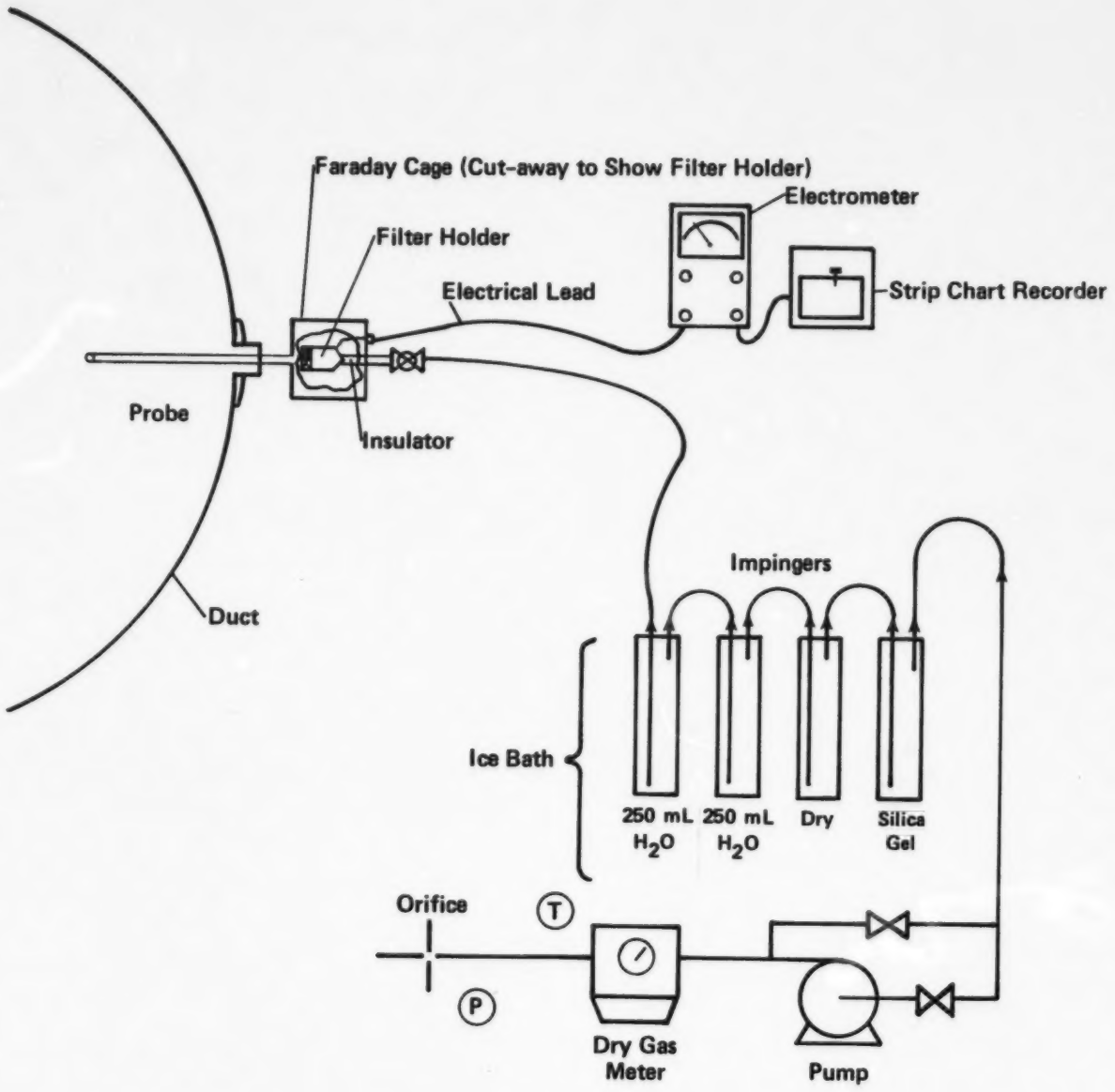

Figure B-1. Charge-to-mass sampling train.